AMÁLIA MARIA SACILOTTO DETONI

FATORES AMBIENTAIS DURANTE FLORAÇÕES FITOPLANCTÔNICAS PRÓXIMAS À ILHA JAMES ROSS, PENÍNSULA ANTÁRTICA (VERÃO- 2008 e 2009)

RIO GRANDE
Agosto de 2010

UNIVERSIDADE FEDERAL DO RIO GRANDE
INSTITUTO DE OCEANOGRAFIA
PÓS-GRADUAÇÃO EM OCEANOGRAFIA BIOLÓGICA

FATORES AMBIENTAIS DURANTE FLORAÇÕES FITOPLANCTÔNICAS PRÓXIMAS À ILHA JAMES ROSS, PENÍNSULA ANTÁRTICA (VERÃO- 2008 e 2009)

AMÁLIA MARIA SACILOTTO DETONI

Dissertação apresentada ao Programa de Pós-Graduação em Oceanografia Biológica da Universidade Federal do Rio Grande, como requisito parcial à obtenção do título de MESTRE.

Orientador: Carlos Alberto Eiras Garcia
Co-orientadora: Virginia Maria Tavano Garcia

RIO GRANDE
Agosto de 2010

AGRADECIMENTOS

Esta dissertação é dedicada aos principais professores da minha vida: meus pais, Vlamir e Maria Aparecida Detoni, e meus orientadores Virginia T. Garcia e Carlos A. E. Garcia. Vocês têm compartilhado comigo suas graças e sabedorias, as quais sempre carrego comigo, transmitindo aos outros o que com vocês tenho aprendido.

Agradeço a Deus, por ter me dado esta oportunidade de estar no mundo.

Agradeço a minha família, principalmente minhas queridas irmãs Aline e Amanda Detoni, por todo o amor, carinho, compreensão e respeito.

Tenho muito a agradecer e a muitas pessoas que me auxiliaram até onde já cheguei....

Meus agradecimentos especiais a:

Às amigas do laboratório e ao Renan, (Amábile, Camila, Karina, Lorena, Ana, Ella e Caju) pela amizade, companheirismo, dedicação e sinceridade nas palavras (esta última é em especial para Lorena e Karina).

Mauricio Cunha, por todos os dias me fazer feliz pelo simples fato de ter cruzado o meu caminho...

Carlos Fujita e Márcio, pelo companheirismo de todos esses anos, desde minha graduação, sempre me incentivando.

Rafael Mendes e Ana Dogliotti, pelos conselhos, conversas e amizade.

Rodrigo Kerr, por me ensinar tudo o que hoje sei do ODV!!!!

Não basta dar os passos que nos devem levar um dia ao objetivo, cada passo deve ser ele próprio um objetivo em si mesmo, ao mesmo tempo em que nos leva para diante.

- Johann Wolfgang Von Goethe

ÍNDICE

RESUMO

Altas concentrações de clorofila-a (Clo-a) são observadas através de imagens de cor do oceano, desde o verão austral de 2003/2004 até o verão de 2008/2009, em águas próximas à Ilha James Ross (IJR), leste da ponta da Península Antártica.

Uma pluma de menor salinidade (< 34,25) encontrada a frente da IJR, provavelmente devido a retração de geleiras de maré*, introduzindo água doce para o oceano, estabiliza a camada superficial da coluna de água formando uma rasa camada de mistura (< 50m) e também contribui com aporte de micronutrientes terrígenos. Amostragens foram conduzidas nos verões de 2008 e 2009 a fim de caracterizar e entender a dinâmica da biomassa fitoplanctônica associada com as condições ambientais próximo à IJR. Um marcado núcleo de águas superficiais com altas concentrações de Clo-a (> $4 mg \cdot m^{-3}$) foi observado por dados coletados no ambiente durante dois verões consecutivos. Este núcleo foi associado com uma camada de mistura rasa (aproximadamente 30m) e temperaturas superficiais relativamente altas (aproximadamente 0,24ºC), principalmente durante o verão de 2009. Neste trabalho, demonstramos que as mudanças espaciais e em magnitude da biomassa fitoplanctônica na área de estudo estão associadas às alterações das condições ambientais locais, bem como à retração das geleiras de maré na IJR, conjuntamente com a retração antecipada da plataforma de gelo do Mar de Weddell. Adicionalmente, a área de estudo apresenta grande influência de icebergs, cuja água de degelo ao redor pode afetar as condições de crescimento do fitoplâncton, pois atua tanto como fonte de nutrientes como no controle da estratificação da coluna de água. Em 19 de fevereiro de 2009 um iceberg foi marcado com uma bóia GPS na plataforma continental do Mar de Weddell. Três das estações oceanográficas foram amostradas ao sul do iceberg e três foram amostradas ao norte. Concluímos que a trajetória de um iceberg pode afetar a coluna de água superior, principalmente em ambientes rasos, podendo perturbar o fundo e revolver o sedimento, ressuspendendo macronutrientes e células do fitoplâncton.

Palavras-chave: geleiras de maré, gelo marinho, floração fitoplanctônica, degelo, profundidade da camada de mistura, estrutura termohalina.

*Definição: geleiras de maré são geleiras que terminam no mar, geralmente em um fiorde (Simões, 2004).

ABSTRACT

In surrounding waters of James Ross Island (JRI), east of Antarctic Peninsula tip, high chlorophyll-a concentration (Chla) has been detected by ocean color imagery, since austral summer of 2003/2004 to summer of 2008/2009.

A plume of low salinity (< 34.25) found in front of JRI, probably due to freshwater input from melting glaciers, stabilizes the upper water column by forming a shallow mixed layer (< 50m) and also contributes with micronutrients from dust and rock material from the Island to sea water. Samplings were conduced in summers 2008 and 2009 in order to characterize and understand the dynamics of phytoplankton biomass associated with the environmental conditions near JRI. A patch of high Chla (> 4mg·m^{-3}) was observed by *in situ* measurements during the two consecutive summer cruises. This patch was associated with shallow upper mixed layer depth (approximately 30m) and relatively high sea surface temperature (approximately 0.24ºC), mainly during summer 2009. The results support the hypothesis that phytoplankton biomass distribution close to JRI may be related to retreat of JRI glaciers. We demonstrated that both magnitude and spatial changes in phytoplankton biomass in the region are associated to local alterations in the environmental conditions, such as retreat of tidewater glaciers in JRI in conjunction with late sea ice shelf retreat. Furthermore, the region presents icebergs influence, whose melting waters may have an effect on growth conditions for phytoplankton because they act as both a source of nutrients and control the stratification of the surface layer. In 19 February 2009 an iceberg was tagged with a GPS buoy on Weddell Sea shelf. Three oceanographic stations were sampled south and three north of the iceberg. We conclude that the icebergs track can affect the water column, mainly in very shallow environments, by disturbing the shallow sea bottom and revolving sediments, resuspending macronutrients and cells of phytoplankton deposited earlier.

Keywords: Tidewater glacier, Sea ice, Phytoplankton bloom, Meltwater, Mixed layer depth, thermohaline structure.

I) INTRODUÇÃO

I.1.) A Distribuição da Biomassa Fitoplanctônica no Oceano Austral

No ambiente oceânico, o fitoplâncton é o principal componente da base da teia trófica, promovendo a ligação entre a energia solar e a produção de recursos biológicos do qual dependem todos os outros níveis tróficos. Portanto, a caracterização temporal e espacial da biomassa fitoplanctônica e produtividade primária tem sido um tópico de grande interesse da comunidade científica oceanográfica. Por sua vez, esta informação é de grande relevância no Oceano Austral (águas ao sul de 50ºS), pois o fitoplâncton, como componente autotrófico do ecossistema marinho, afeta a estrutura e eficiência da teia trófica, ciclos biogeoquímicos globais, e a bomba biológica do CO_2 (Garibotti *et al.*, 2005).

O Oceano Austral é caracterizado por apresentar grande disponibilidade de macronutrientes, que deveria sustentar uma alta produtividade primária. Entretanto, geralmente, as concentrações de clorofila-a e a produtividade primária no Oceano Austral são típicas de um oceano oligotrófico para mesotrófico (Fiala *et al.*, 1998; Garibotti *et al.*, 2005). Altas concentrações de clorofila-a são encontradas em algumas regiões do Oceano Austral associadas principalmente às regiões costeiras, *polyneas**, bordas do gelo marinho, ilhas e regiões de frentes oceanográficas (Smith & Nelson, 1990, Garibotti *et al.*, 2003, Arrigo & Dijken, 2004, Smith & Comiso, 2008).

O crescimento do fitoplâncton no Oceano Austral é controlado por muitos fatores, como: disponibilidade de luz, cobertura de gelo e ventos, disponibilidade de ferro e herbivoria pelo zooplâncton (Holm-Hansen *et al.*, 1989, Mitchell *et al.*, 1991, Constable & Nicol, 2003, Marrari *et al.*, 2008). Porém, o grau com que os fatores

*Definição: *polyneas* são áreas de água aberta cercada por gelo marinho.

físicos, químicos e biológicos podem limitar o crescimento fitoplanctônico ainda não está completamente entendido, e sua importância pode variar conforme a localização, tempo e condições meteorológicas locais (Lancelot *et al.*,1993).

Modelos prévios teóricos; e empíricos, sugerem que a estabilidade da coluna de água, herbivoria e/ou limitação por algum recurso, como o metal traço ferro, são os principais fatores que governam a dinâmica das florações fitoplanctônicas (Michell & Holm-Hansen, 1991). Enquanto essas investigações têm avançado no entendimento dos mecanismos que controlam a dinâmica fitoplanctônica, também apontam a necessidade de estudos com melhor resolução espacial destes processos físico-biológicos.

Recentemente, muitos estudos têm indicado que a produtividade primária oceânica na Antártica é limitada pela deficiência do micronutriente ferro, sendo encontrados níveis muito baixos de ferro em águas oceânicas com baixa biomassa, onde a concentração de nutrientes é praticamente constante (Martin *et al.*, 1991, Boyd *et al*., 2002). Porém, alta biomassa fitoplanctônica é encontrada próxima ao aporte do ferro, como ilhas, plataformas continentais (aporte continental) e frentes oceanográficas (ressurgência), a partir da primavera com o derretimento do gelo continental e marinho (Martin *et al*., 1991, Loscher *et* al., 1997, Holm-Hansen *et al*., 2004).

A estabilidade da coluna de água é um dos primeiros fatores que regulam a concentração de fitoplâncton em águas de superfície da Antártica durante o verão austral (Michell & Holm-Hansen, 1991, Garibotti *et al*., 2003, Hewes *et al*., 2008). Esta característica está associada com a profundidade da camada de mistura vertical na coluna de água superior, que impede a sedimentação das células do fitoplâncton, permitindo que permaneçam na coluna de água sob condições de luz favoráveis (Mitchell & Holm-Hansen, 1991, Garibotti *et al*., 2005, Vernet *et al*., 2008).

Assim como observado por Hewes *et al*. (2008), as maiores biomassas de fitoplâncton ocorrem sob condições com abundância de macronutrientes e metais traços, profundidade da camada de mistura variando entre 25 e 50 metros e salinidades intermediárias (~34), durante o verão austral nas Ilhas Shetland do Sul, a oeste da Península Antártica. Entretanto, pouco é conhecido sobre a dinâmica do fitoplânton nas águas próximas à Ilha James Ross, a leste da Península Antártica. Estudos recentes observam que, á oeste da Península Antártica, a variabilidade espacial e temporal dos processos sazonais de extensão e retração do gelo marinho e continental, reflete na dinâmica das populações fitoplanctônicas, atuando de forma significativa na substituição de espécies adaptadas ao gelo por espécies competitivas, assim interferindo em toda uma cadeia trófica biogeográfica (Montes-Hugo *et al*., 2009). É necessário obter maiores investigações para o leste da Península Antártica, onde ainda não tem sido observado o mecanismo da biomassa do fitoplâncton associada às mudanças ambientais locais. Nesta região, as florações fitoplanctônicas, provavelmente seguem um gradiente horizontal de salinidade, como encontrado por Hewes *et al*. (2008) a oeste da Confluência Weddell-Scotia. A região leste da Península Antártica apresenta grande influência das águas salinas do Mar de Weddell (Piatkowski, 1989, Gordon *et al*., 2000), que se misturam com água de degelo continental da Ilha James Ross.

I.2.) Os Efeitos do Gelo Marinho Antártico sobre as Florações Fitoplanctônicas

O derretimento do gelo marinho, na sua zona marginal, propicia condições favoráveis para o aumento da produtividade primária e biomassa fitoplanctônica, por atuar como fonte de macro e micro nutrientes (incluindo o ferro, dependendo de sua formação) (Martin *et al*., 1991, Loscher *et al*., 1997, Sedwick & DiTullio, 1997) e produzir uma camada de mistura rasa através da estratificação das águas superficiais (Boyd, 2002, Garibotti *et al*., 2003, Marrari *et al*., 2008). O gelo marinho pode acumular ferro a partir da deposição atmosférica de poeira mineral (Edwards & Sedwick, 2001), e também pode incorporar o ferro através de fontes sedimentares quando formado em regiões costeiras ou plataforma continental (Sedwick *et al.*, 2000, Fitzwater *et al.*,2000, Grotti *et al*., 2005).

A zona marginal do gelo no Mar de Weddell é considerada como uma das regiões mais produtivas do Oceano Austral (Kang *et al*., 2001, Arrigo *et al*., 2008). Durante o verão, as águas de degelo desta zona marginal, proporcionam condições físico-químicas na coluna de água favorecendo o crescimento do fitoplâncton. Dados de satélite indicam que a cobertura sazonal do gelo marinho nesta região começa a diminuir a partir do final de novembro, e séries temporais mensais mostram este derretimento progredindo rapidamente durante o verão (Kang *et al*., 2001).

Através de imagens da cor do oceano, é possível observar, próximo a esta margem do gelo, o início das florações de fitoplâncton sazonais, a qual se move progressivamente em direção sul, intensificando a partir de dezembro até fevereiro (Holm-Hansen *et al*., 2004). Entretanto, o período em que se inicia esta floração e sua magnitude apresenta variações anuais, podendo ser dependente da persistente cobertura de gelo, profundidade da camada de mistura e da radiação solar incidente (Smith & Comiso, 2008). Em uma investigação das mudanças interanuais na dinâmica do gelo marinho e forçantes meteorológicas no sudoeste do Mar de Ross, relacionadas ao impacto no ciclo anual da abundância do fitoplâncton, Arrigo & van Dijken (2004) mostram que a quantidade de gelo no Mar de Ross, está também relacionada ao grau de cobertura de nuvem, a qual, por sua vez, pode também afetar as taxas interanuais de produção primária, devido à menor disponibilidade de luz.

Mudanças na dinâmica da cobertura do gelo marinho devido ao aquecimento do ar (retração antecipada do gelo marinho) não afetam diretamente a composição do fitoplâncton antártico, mas induzem à instabilidade na dinâmica do ciclo sazonal do fitoplâncton, com impactos na cadeia trófica (Garibotti *et al.*, 2005). Entretanto, Montes-Hugo *et al*. (2009) demonstraram que, a oeste da Península Antártica, há diferentes tendências na concentração da clorofila-a, provavelmente acompanhadas pelas mudanças na composição das comunidades do fitoplâncton. Uma fração maior de diatomáceas microplanctônicas é observada na região sul, onde a diminuição da extensão do gelo marinho tem ocorrido em áreas que anteriormente eram cobertas por gelo na maior parte do ano.

I.3.) Os Efeitos dos Icebergs nas Florações Fitoplanctônicas

Os icebergs têm sido estudados como fonte de micronutrientes para águas oceânicas oligotróficas do Oceano Austral (Arrigo & Dijken, 2004, Schodlok *et al*., 2006, Schwarz & Schodlok, 2009). Esses se desprendem das plataformas de gelo e derivam por águas oceânicas do Oceano Austral, liberando água doce, sedimentos terrígenos e micronutrientes em áreas que apresentam baixa produtividade primária, proporcionando assim condições favoráveis para o crescimento do fitoplâncton em zonas pelágicas (Arrigo & Dijken, 2004, Smith *et al*., 2007, Schwarz & Schodlok, 2009). Porém, o impacto causado pelos icebergs em águas ao seu redor, ainda é pouco conhecido e estudado através de dados coletados *in situ*. Observações casuais sugerem que tanto a depleção como o enriquecimento de compostos químicos e as conseqüências para os processos biológicos em zonas pelágicas, podem estar associadas com a passagem dos icebergs (Smith *et al*., 2007, Schwarz & Schodlok, 2009). No entanto, existem alguns mecanismos pelos quais os icebergs podem causar impactos potencialmente negativos na produtividade primária superficial. Embora a água de degelo liberada pelo derretimento do iceberg possa aumentar a estabilidade da camada de mistura superficial, uma vez à deriva, a quilha do iceberg, sendo muito profunda, pode provocar mistura na coluna de água e perturbar a estabilidade da camada superficial.

A desintegração de plataformas de gelo em ambos os lados da Península Antártica durante os últimos 60 anos, tem sido atribuída ao aquecimento atmosférico, e tem contribuído para o aumento freqüente de icebergs no Mar de Weddell, próximo à Península Antártica (Smith *et al*., 2007).

II.) Área de Estudo

A Ilha James Ross (IJR) está localizada à nordeste da Península Antártica. A Ilha abrange 80 km de norte a sul e 70 km de leste a oeste. Aproximadamente 80% da Ilha está coberta por geleiras (Sone *et al*., 2007). A Ilha recebe abundante precipitação, mas a cobertura derrete significativamente nos meses de verão e é drenada pelos rápidos fluxos que escoam das geleiras (Hawes & Brazier, 1991; Sone *et al*., 2007). A existência de lagos glaciais originados por erosão do alto das geleiras observados durante o verão austral 2004-2005 na IJR foram relatados por Sone *et al*. (2007). Esses lagos são geralmente reconhecidos como resultado do aquecimento climático, o qual está sendo recentemente relatado nesta região (Sone *et al*., 2007, Hawes & Brazier, 1991). Condições topográficas da IJR podem fazer com que os fluxos de degelo sigam em direção ao ambiente marinho, como observado por Hawes & Brazier (1991).

As águas próximas à IJR são influenciadas pela dinâmica e circulação da Água de Plataforma do Mar de Weddell (APMW), a qual transporta grande carga de nutrientes e ferro que são liberados através do derretimento da plataforma de gelo e conduzidos para regiões costeiras e pelágicas (Kang *et al*., 2001). Adicionalmente, esta região é caracterizada pela abundante presença de icebergs e pelos fluxos de água doce das geleiras de maré da Ilha, que escoam para a superfície do oceano.

Devido à presença de altos valores de nutrientes e metais traços, como o ferro, e à alta estabilidade da coluna de água, esta região apresenta condições propícias para uma alta biomassa e produtividade fitoplanctônica, onde Kang *et al*. (2001) observaram que as concentrações de nutrientes são inversamente relacionadas com a biomassa fitoplanctônica, apresentando depleção de nitrato (10µM) e silicato (50µM) e altos valores de clorofila-a ($10 mg \cdot m^{-3}$).

À frente da IJR, o ecossistema marinho é regulado pela variação sazonal e influenciado pela margem do gelo marinho, a qual é controlada pela dinâmica (retração e avanço) da plataforma de gelo do Mar de Weddell, apresentando alta biomassa e produtividade fitoplanctônica (Kang *et al*., 2001). A liberação potencial de nutrientes, além da estabilidade da coluna de água em superfície, favorece a floração sazonal do fitoplâncton nesta região, que é normalmente observada através de imagens de satélite da cor do oceano.

Existem muitos estudos sobre a variabilidade espacial e sazonal da dinâmica e estrutura do fitoplâncton antártico a oeste da Península Antártica, principalmente pelos programas amostrais de longa duração, baseados na estação Antártica Norte-americana (Holm-Hansen & Michell, 1991, Mitchell & Holm-Hansen, 1991, Kang *et al*., 2001, Garibotti *et al*., 2003, Garibotti *et al*., 2005, Marrari *et al*., 2006, Marrari *et al*., 2008, Vernet, *et al*., 2008).

Porém pouco se conhece sobre sua variabilidade e estabilidade interanual na parte leste da Península. A floração fitoplanctônica, geralmente observada na região nordeste da Península Antártica, tem importante implicação para o entendimento do ecossistema marinho antártico, a qual tem influência determinante nos níveis de CO_2 atmosférico, sendo capaz de responder às variações das condições ambientais através da variabilidade interanual e dinâmica espacial das comunidades do fitoplâncton (Garibotti *et al*., 2003).

III.) Objetivos do Trabalho

No presente trabalho, propusemos estudar os fatores ambientais associados às florações fitoplanctônicas à leste da Península Antártica, nas proximidades da Ilha James Ross, onde geralmente altos valores de concentração de clorofila-a são observados por imagens de satélite da cor do oceano, com o objetivo de comparar as florações fitoplanctônicas observadas durante dois anos consecutivos, e verificar possíveis mudanças ambientais que possam afetar a produtividade local.

Para atingir o objetivo central, o NAp. Oc. Ary Rongel amostrou a região durante dois anos consecutivos, onde foram medidas as propriedades físicas, óticas e biogeoquímicas, a fim de caracterizar as condições ambientais durante as florações fitoplanctônicas (mar. 2008 e fev. 2009).

Adicionalmente, com a finalidade de verificar as mudanças ambientais na água do mar ao redor de icebergs, um estudo pioneiro brasileiro foi conduzido na Antártica. Um iceberg foi marcado por uma bóia GPS e sua posição diária foi determinada através de imagens de satélite e pelo sistema GPS. Este iceberg estava localizado na plataforma continental do Mar de Weddell, onde foram realizadas estações oceanográficas ao seu redor, com medições físicas, químicas e biológicas. Este experimento foi realizado com o objetivo de observar o impacto da presença de um iceberg na coluna de água adjacente e em superfície e, assim, inferir possíveis conseqüências na produtividade primária local.

A hipótese central deste presente trabalho é de que o degelo continental, originado da IJR, e do continente próximo à área de estudo, que escoa para o oceano, adicionado à dinâmica de avanço e retração anual do gelo marinho, sejam os principais determinantes físicos das mudanças espaciais e temporais das florações fitoplanctônicas nas proximidades da IJR.

Nesta seção do trabalho será apresentado um resumo da metodologia e dos principais resultados encontrados. A seguir, nos apêndices, são apresentados dois manuscritos, extraídos desta dissertação, que serão submetidos como artigos em periódicos científicos.

IV) MATERIAL E MÉTODOS

Os cruzeiros oceanográficos foram conduzidos em dois verões de dois anos consecutivos: 2008 (1 a 3 de março) e 2009 (17 a 20 de fevereiro), como parte do Projeto "Southern Ocean Studies for Understanding Global Climate Issues (SOS-CLIMATE)", no âmbito da contribuição brasileira para o IV API (Ano Polar Internacinal).

A área amostrada foi nas proximidades da IJR. O número de estações realizadas com o sistema Roseta/CTD durante os cruzeiros foram: 20 estações no SOS I (2008) e 12 estações no SOS II (2009) (figura 1).

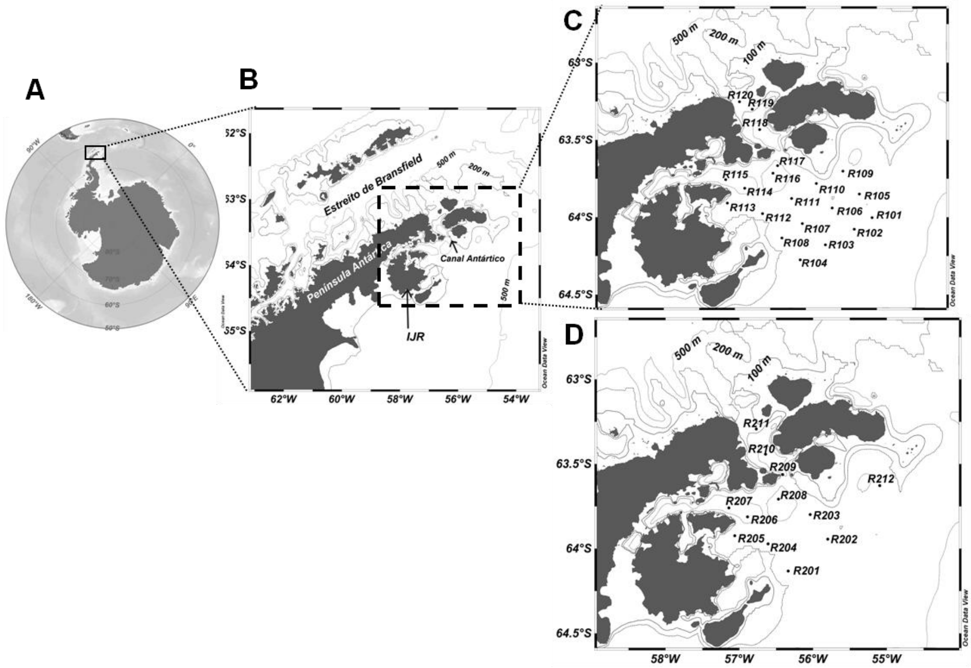

Figura 1. (A) Continente Antártico destacando a extremidade da Península Antártica. (B) Área de estudo. (C) Localização das estações hidrográficas durante o verão de 2008. (D) Localização das estações hidrográficas durante o verão de 2009 (D).

Em 19 de fevereiro de 2009 um iceberg marcado foi escolhido visualmente através de um helicóptero e, a bóia GPS associada ao sistema satélite ARGOS, foi posicionada ao centro do iceberg na posição 64°14,45'S e 55°27,10'W (figura 2). O iceberg era de forma tabular com aproximadamente 1.78km de comprimento e 1.39km de largura.

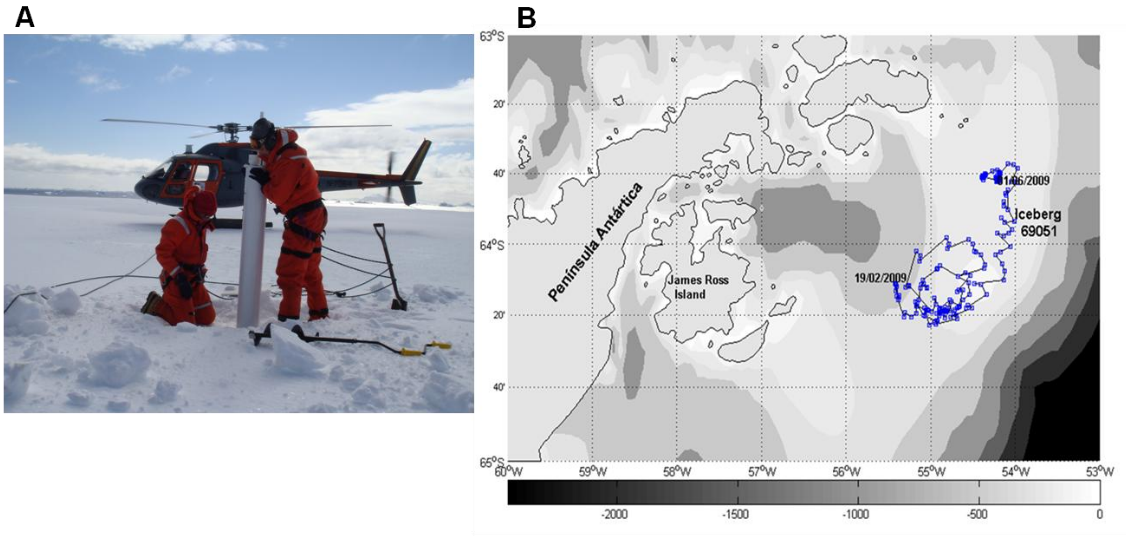

Figura 2. (A) Foto da colocação do transdutor no iceberg. (B) Trajetória do iceberg a partir de 19 de fevereiro de 2009 a 1 de junho de 2009, posição enviada pelo transdutor.

IV.1.) Dados oceanográficos

Perfis verticais de temperatura, salinidade, fluorescência e atenuação da luz (660nm) foram realizados utilizando o sistema Sea-Bird CTD/Carrousel 911+. Foram consideradas as medidas de temperatura, salinidade e pressão realizadas durante a perfilagem de descida do CTD/Carrousel, enquanto para a fluorescência estimulada e atenuação da luz foram utilizadas as medidas da perfilagem de subida do CTD. Este procedimento foi determinado pelo fato das amostras de água, que serviram para análises da concentração da clorofila-a, terem sido coletadas durante a subida do CTD. Assim, espera-se encontrar melhor precisão e acurácia na relação entre os dados de concentração de clorofila-a e propriedades óticas medidas através de sensores acoplados ao sistema CTD/Carrousel.

Foram realizadas correções para calibração do instrumento, devido a sua deriva ou incrustações, através de dados de referência de atenuação da luz. Nas estações mais profundas de cada cruzeiro, foi encontrado o valor constante de atenuação da luz em cada cruzeiro, medidos nas profundidades de ~2100–2200m, onde não são encontradas células do fitoplâncton. Esses valores de atenuação da luz, correspondente a cada cruzeiro, foram subtraídos de todos os valores do conjunto de dados de atenuação da luz, considerando estes valores um *offset* dentro dos dados. O cruzeiro SOS-I apresentou um *offset* de $0.04m^{-1}$, e o SOS-II um *offset* de $0.17m^{-1}$. Este procedimento foi aplicado a fim de obtermos os valores de atenuação da luz apenas para o material particulado em 660 nm.

A fluorescência estimulada medida *in situ* foi utilizada como um índice da biomassa do fitoplâncton, a partir da correlação linear obtida entre fluorescência e concentração de clorofila-a ($r=0.86$, $p<0.001$ e $n=32$).

IV.2.) Medida dos pigmentos do fitoplâncton

As concentrações de clorofila-a foram obtidos através de Cromatografia Líquida de Alta Performance (HPLC). Amostras de água foram filtradas em filtros Whatman GF/F de25 mm de diâmetro, imediatamente estocados em nitrogênio líquido. A análise foi realizada por MSc. Carlos Rafael Mendes no Centro de Oceanografia, da Faculdade de Ciências da Universidade de Lisboa, segundo o método descrito em Mendes *et al*. (2007).

IV.3.) Profundidade da Camada de Mistura

A profundidade da camada de mistura foi determinada como a profundidade onde, no perfil da densidade potencial, esta difere 0.02kg·m^{-3} a partir do valor da densidade potencial média encontrada no intervalo de 5 a 10 m (adaptado de Hewes *et al*., 2008). Este valor diferencial da densidade (0.02kg·m^{-3}) foi determinado a partir da máxima diferença encontrada ao longo do perfil na coluna de água, ou seja, onde a variação da densidade entre uma profundidade e a densidade da profundidade seguinte era máxima. Para o experimento realizado nas proximidades do iceberg, a densidade diferencial considerada foi 0.08kg·m^{-3}.

IV.4.) Dados de satélites

Para análise da variabilidade da concentração de clorofila-a (em escala logarítmica), foram utilizadas imagens médias mensais, SMI (*Standard Mapped Image*) Level-3, do sensor MODIS-Aqua (*Moderate Resolution Imaging Spectroradiometer - Aqua*), com resolução espacial de 4X4 km, cujos dados já processados são disponíveis disponibilizado pela NASA (*http://oceancolor.gsfc.nasa.gov*).

Imagens diárias de concentração de gelo foram obtidas para a composição de uma imagem mensal. O período escolhido foi de Outubro a Março para os anos de 2002 a 2009. Os dados foram coletados pelo sensor AMSR-E (*Advanced Microwave Scanning Radiometer for EOS*) com resolução espacial de aproximadamente 6x4 km no canal de freqüência 89 Ghz. O algoritmo *Artist Sea Ice* (ASI) é aplicado sobre os valores de temperatura de brilho, o qual utiliza um modelo empírico para estimar a concentração do gelo entre 0% e 100% (Spreen *et al*., 2008) em cada pixel. Mapas hemisféricos diários de concentração de gelo utilizando o algoritmo ASI são operacionalmente publicados no Institute of Environment Physics da Universidade de Bremen (*www.iup.physik.uni-bremen.de*).

As áreas médias mensais de gelo marinho, de água sem cobertura de nuvens e de água coberta por nuvens, dentro da área oceânica de estudo para o período analisado, foram determinadas utilizando o conjunto de imagens MODIS-Aqua e AMSR-E. A área sob investigação possui coordenadas variando de 64,5°S a 63,2°S de latitude e de 57,7°W a 54°W de longitude, nas proximidades da IJR. Para cada mês, os pixels de água sem nuvens foram identificados através do algoritmo ASI, onde a concentração de gelo no pixel fosse inferior ou igual a 15%, sendo este limite geralmente definido como borda do gelo (Marrari *et al*., 2008, Spreen *et al*., 2008). A área de gelo marinho foi determinada pelos pixels que continham concentração de gelo superior a 15%, este limiar mantém todas as concentrações de gelo acima das concentrações as quais representam a zona marginal do gelo. Imagem MODIS-Aqua para o mesmo mês foi então comparada com a imagem AMSR-E. Qualquer pixel do MODIS-Aqua sobre a água sem nuvens (definida acima) que foi mascarado (não contem dado) como sendo gelo marinho ou nuvem foi assumido como cobertura de nuvem sobre a região oceânica.

A resolução espacial do pixel do sensor AMSR-E foi determinada pela área do número total de pixels definida a partir da resolução espacial do pixel na imagem MODIS-Aqua. A área total foi dividida pelo número total de pixels da imagem AMSR-E.

V) RESULTADOS

V.1) Dados de concentração de clorofila-a (MODIS-Aqua) e concentração de gelo (AMRS-E)

A série temporal da concentração média de clorofila-a (Clo-a) mensal estimada pelo sensor MODIS entre os meses de outubro a março (verão austral), no período de 2002 a 2009 mostra picos com maiores Clo-a (> $1 mg \cdot m^{-3}$) nos meses de janeiro e fevereiro (ver Apêndice 1, figura 2). Esta variabilidade interanual da Clo-a está associada provavelmente com a cobertura de gelo sazonal e outras condições ambientais (como a nebulosidade local); entretanto, a ausência de dados na imagem devido à cobertura de nuvens, pode, em parte, explicar a variabilidade observada. Devido ao crescimento inicial do fitoplâncton numa floração fitoplanctônica ser fortemente controlado pela disponibilidade de luz, surgiu o interesse em determinar a existência de uma diferença significativa interanual na cobertura de nuvens, o que pode reduzir a incidência de luminosidade em mais de 50% (Arrigo & van Dijken, 2004). Assim, as diferenças na fração de cobertura de nuvens durante os sete verões analisados para a área de estudo, podem ser relacionadas com as mudanças na biomassa fitoplanctônica em frente à IJR.

Foram encontradas as frações que cada componente (oceano, gelo e nuvem) contribui para as suas respectivas variações em áreas para todos os meses (outubro a março) do verão austral e para todos os anos analisados (2002 a 2009), estimadas pelo sensor MODIS (figura 3). Conjuntamente, foram observados os dados de satélite da concentração de gelo dos meses de janeiro e fevereiro de 2008 e 2009, mostrando que em 2009 houve relativamente maior área livre de gelo marinho do que 2008 (ver Apêndice 1, figura 4).

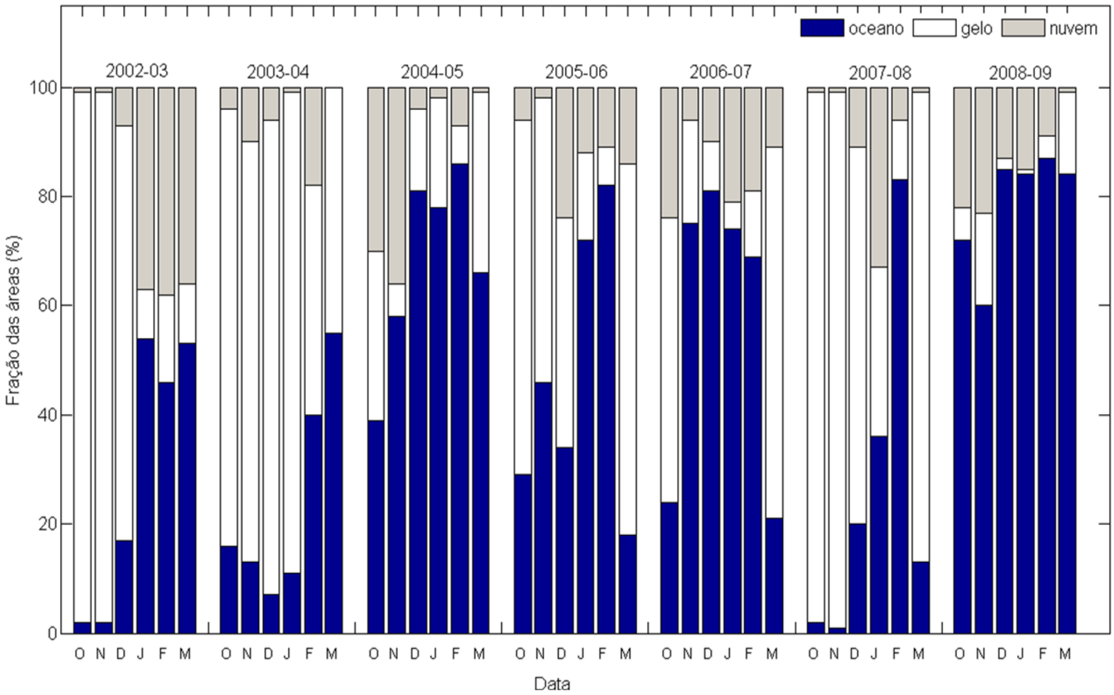

Figura 3. Frações das áreas de água coberta por nuvem (cinza), água sem nuvem e livre de gelo (azul) e gelo marinho (branco).

Isto sugere que, a ausência (ou presença) de gelo marinho pode ser resultado da elevação (ou diminuição) na incidência de radiação solar durante um verão austral onde a cobertura de nuvem é menor (ou maior), levando ao aquecimento (resfriamento) da superfície do mar e maior (menor) derretimento do gelo marinho, assim controlando a dinâmica da cobertura de gelo e de área de oceano exposto (Jacobs & Comiso, 1989, Arrigo & van Dijken, 2004). Esta conexão poderá implicar numa alteração na dinâmica do crescimento fitoplanctônico e produtividade primária a leste da Península Antártica, como demonstrado por Montes-Hugo *et al*. (2009) em estudo na região oeste da Península Antártica.

V.2) Dados *in situ*

Os perfis do diagrama T/S dos cruzeiros de 2008 e 2009 mostraram maiores valores de temperatura potencial para todas as estações do cruzeiro de 2009 (Apêndice 1, figura 5). Este aumento na temperatura da água foi de aproximadamente 0,5ºC ao longo da coluna de água amostrada durante o cruzeiro de fevereiro de 2009. Para análise dentro da camada de mistura, foi observada água de menor salinidade (< 34,25) e menor temperatura potencial nas estações logo a frente da IJR, para ambos os cruzeiros amostrados (2008 e 2009) (Apêndice 1, figura 5). Isto indica que esta área foi influenciada por água de degelo, que estaria sendo advectada pelo fluxo das geleiras da ilha para o oceano.

A distribuição das águas de superfície (Apêndice 1, figura 6) também denota menores salinidades (< 34,25) e temperaturas (< 0,60°C) na área a frente da Ilha. Este processo leva a maior estratificação da coluna de água, pela presença de água com menor densidade, conduzindo a uma menor profundidade da camada de mistura superior, condição esta favorável ao crescimento do fitoplâncton. A profundidade da camada de mistura superior (UML) encontrada variou entre 23–50m nas estações próximas à IJR, e foram maiores que 100 m dentro do Canal Antártico (CA). Porém, foram observadas menores profundidades da UML (23–29m), principalmente no cruzeiro de 2009, em relação ao cruzeiro do ano anterior.

A ocorrência de uma floração fitoplanctônica à frente da IJR mostrado na figura 4, com maiores valores de fluorescência estimulada, Clo-a e atenuação da luz, observadas nos gráficos (A), (B) e (C), respectivamente, representando o cruzeiro SOS I, e (D), (E) e (F) representando o cruzeiro SOS II. Estas florações, que são geralmente observadas sazonalmente através de imagens de cor do oceano, e que foram também amostradas pelos cruzeiros, são influenciadas pelo aumento da estabilidade da coluna de água, criada pelo degelo das geleiras, onde a água doce, ao fluir para o oceano, forma camada de mistura rasa. Esta região também é abrigada dos ventos de oeste, o que contribui para que a estabilidade da coluna de água permaneça por mais tempo, sem que a cobertura de vento provoque turbulência e mistura na coluna de água. O aporte de micronutrientes terrígenos, como o ferro, provavelmente ocorre, criando assim condições favoráveis para que ocorra a floração próxima à IJR, observada em nossos cruzeiros.

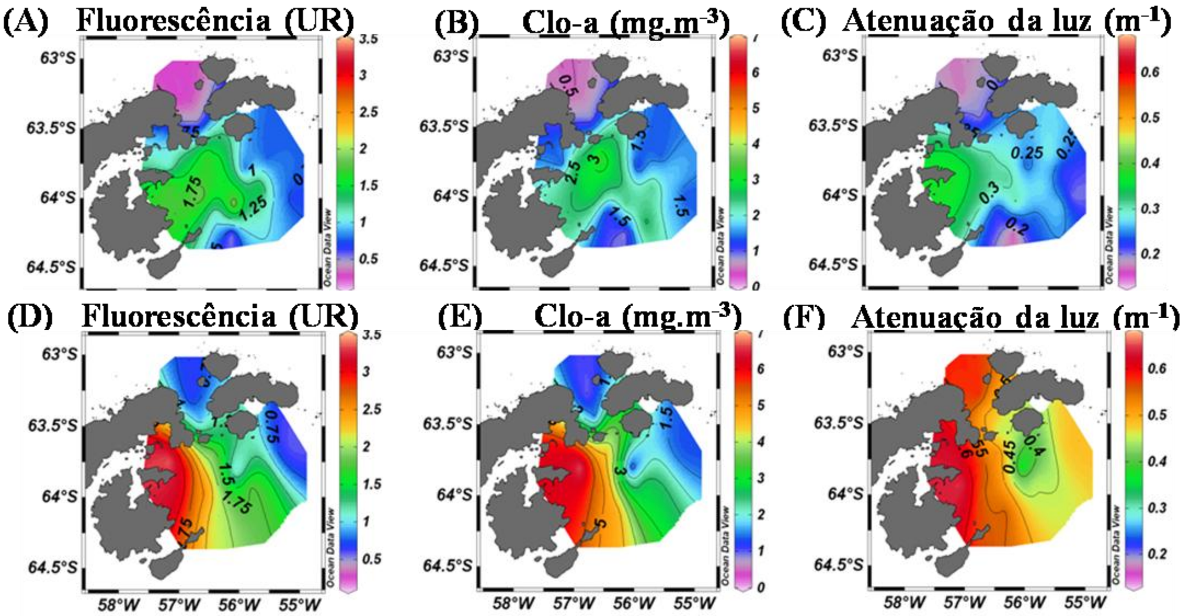

Figura 4. Distribuição superficial dos parâmetros biológicos fluorescência (unidade relativa – UR), concentração da clorofila-a (Clo-a – mg.m^{-3}) e atenuação da luz (m^{-1}) durante os cruzeiros conduzidos no verão de 2008 (A,B e C) e verão de 2009 (D, E e F).

Adicionalmente, observamos uma correlação significativa entre a Clo-a e salinidade para os consecutivos verões amostrados. Para ambos os cruzeiros, a relação entre a salinidade da água e a Clo-a apresentaram altos coeficientes de correlação negativos, -0.80 para SOS I e -0.81 para SOS II. Esta correlação inversa apóia a hipótese de que o aumento da contribuição de águas de baixa salinidade favorece o desenvolvimento da floração fitoplanctônica próxima à IJR. O deságüe de geleiras continentais, como enfatizado acima, contribui para a estratificação das águas superficiais e para o aporte de micronutrientes, como o ferro, que são fatores condicionantes para essas observadas florações (Apêndice 1, para maiores detalhes).

V.3) Propriedade físicas e biológicas observadas ao sul e ao norte de um iceberg

Os dados físicos e biogeoquímicos analisados ao redor do iceberg indicam que, provavelmente, as características ambientais amostradas são conseqüências da passagem do mesmo. Assim, a comparação entre os perfis físicos e biogeoquímicos das estações sul e norte caracterizaram o impacto causado posteriormente à passagem do iceberg (estações ao sul) e o impacto anterior à sua passagem (estações ao norte).

Ao norte do iceberg, a estrutura termohalina apresentou instabilidade na coluna de água superior, com presença de água misturada nas estações mais próximas ao iceberg (ver Apêndice 2, figura 6). Estas estações estão associadas à camada de mistura mais profunda (60-90m). Ao sul do iceberg foi observada uma coluna de água estável e com menor profundidade da camada de mistura (40-50m).

Os perfis verticais para as seis estações amostradas mostraram maiores concentrações de clorofila-a, fluorescência induzida, atenuação da luz, silicato e nitrato em águas profundas (abaixo de 150m), principalmente nas estações ao sul do iceberg, provavelmente após sua trajetória.

As alterações nas propriedades físicas da coluna de água provocadas pela presença do iceberg são inicialmente observadas logo a frente de sua trajetória. Nas estações ao sul, provavelmente após sua passagem, a coluna de água restabeleceu à estabilidade devido à presença de águas menos salinas do rastro do iceberg originadas do seu contínuo degelo. Adicionalmente, as propriedades químicas e biológicas, provavelmente sofreram influência do fundo por ressuspensão, durante o arrasto provocado pela passagem do iceberg, permanecendo nesta condição por maior tempo (ver Apêndice II, para maiores detalhes).

VI) CONSIDERAÇÕES FINAIS

A dinâmica do gelo marinho parece ter uma grande influência sobre o fitoplâncton costeiro na Antártica (Smith *et al*., 1998; Garibotti *et al*., 2003; Arrigo *et al*., 2008). Entretanto, como demonstrado por Garibotti *et al.* (2003), a variabilidade da biomassa fitoplanctônica também depende dos diferentes parâmetros ambientais locais, como as condições físicas da coluna de água e a disponibilidade de ferro.

À frente da IJR, ao elevar sazonalmente a temperatura da superfície do mar, há uma maior área de oceano livre de gelo e, por conseqüência, maior derretimento de geleiras da IJR. O deságüe das geleiras para águas oceânicas estabiliza a camada superior da coluna de água, um importante mecanismo físico para a manutenção do fitoplâncton na camada fótica além de, provavelmente, disponibilizar compostos de ferro, favorecendo seu crescimento. No entanto, este processo é modulado pela maior ou menor presença de nuvens a cada ano, induzindo variabilidade interanual na magnitude das florações fitoplanctônicas.

O aumento relativo da temperatura da superfície do mar diminui a profundidade da camada de mistura superior, com conseqüências para as florações de fitoplâncton. A variabilidade da Clo-a para a área de estudo foi primeiramente detectada através das imagens de satélite da cor do oceano, e posteriormente confirmada pelos dados coletados no ambiente durante os cruzeiros SOS I e SOS II.

Nossos resultados *in situ* caracterizam a variabilidade da biomassa fitoplanctônica em dois anos consecutivos. Esta variabilidade ocorreu como resposta das alterações ambientais locais, como, provavelmente, maior fluxo de degelo das geleiras na IJR próximas ao oceano e aumento da área de oceano exposto livre de gelo marinho durante o segundo cruzeiro de verão (2008-2009), promovendo maiores níveis de biomassa do fitoplâncton em relação ao ano anterior.

A influência de icebergs no Oceano Austral pode perturbar a estrutura termohalina à frente de sua trajetória, provocando turbulência e mistura na coluna de água superior, principalmente em regiões muito rasas, como áreas costeiras e plataforma continental. Nessas regiões, dependendo das dimensões do iceberg, a parte submersa do mesmo pode arrastar o fundo do oceano ao derivar, assim revolvendo o sedimento e ressuspendendo macronutrientes, como silicato e nitrato, e células de microalgas com pigmentos fotossintetizantes ativos, que foram depositados anteriormente.

VII) LITERATURA CITADA

ARRIGO, K. R. & VAN DIJKEN, G. L. 2004. Annual changes in sea-ice, chlorophyll *a*, and primary production in the Ross Sea, Antarctica. *Deep-Sea Research Part **II.*** 51: 117-138.

ARRIGO, K. R., DIJKEN, G. L. & BUSHINSKY, S. 2008. Primary production in the Southern Ocean, 1997 - 2006. *Journal of Geophysucal Research*. 113(C08004): 1 - 27.

BOYD, P. W. 2002. Environmental Factors Controlling Phytoplankton Processes in the Southern Ocean. *Jounal Phycology: An international Journal of Algal Research*. 38: 844-861.

CONSTABLE, A. J. & NICOL, S. 2003. Southern Ocean productivity in relation to spatial and temporal variation in the physical environment. *Journal of Geophysical Research*. 108 (C48079): 1-21.

EDWARDS, R. & SEDWICK, P. 2001. Iron in East Antarctic snow: Implications for atmospheric iron deposition and algal production in Antarctic waters. *Geophysical Research Letters*. 28: 3907-3910.

FIALA, M., KOPCZYNSKA, E. E., JEANDEL, C. & ORIOL, L., VETION, G. 1998. Seasonal and interannual variability of size-fractioned phytoplankton biomass and commumity structure at station Kerfix, off the Kerguelen Island, Antarctica. *Journal of Plankton Research*. 20(07): 1341-1356.

FITZWATER, S. E., JOHNSON, K. S., GORDON, R. M., COALE, K. H. & SMITH Jr, W. O. 2000. Trace metal concentrations in the Ross Sea and their relationship with nutrients and phytoplankton growth. *Deep-Sea Research II*. 47: 3159-3179.

FRANK, H. A., CUA, A., CHYNWAT, V., YOUNG, A., GOSZTOLA, D. & WASIELEWSKI, M. R. 1994. Photophysics of the carotenoids associated with the xantophyll cicles in photosynthesis. *Photosynthesis Research*. 41: 389-395.

GARIBOTTI, I. A., VERNET, M., FERRARIO, M. E., SMITH, R. C., ROSS, R. M. & QUETIN, L. B. 2003. Phytoplnakton spatial distribution patterns along the western Antarctic Peninsula (Southern Ocean). *Marine Ecology Progress Series*. 261: 21-39.

GARIBOTTI, I. A., VERNET, M., SMITH, R. C. & FERRARIO, M. E. 2005. Interannual variability in the distribution of the phytoplankton standing stock across the seasonal sea-ice zone west of the Antarctic Peninsula. *Journal of Plankton Research*. 27(8): 825-843.

GORDON, A. L. & MENSCH, M. 2000. Deep and bottom water of Bransfield Strait eastern and central basins. *Journal of Geophysical Research*. 105 (C5): 11337-11346.

GROTTI, M., SOGGIA, F., IANNI, C. & FRACHE, R. 2005. Trace metals distributions in coastal sea ice of Terra Nova Bay, Ross Sea, Antarctica. *Antarctic Science*. 17(2): 289-300.

HAWES, I. & BRAZIER, P. 1991. Freshwater stream ecosystems of James Ross Island, Antarctica. *Antarctic Science.* 3(3): 265-271.

HEWES, C. D., REISS, C. S., KAHRU, M., MITCHELL, B. G. & HOLM-HANSEN., O. 2008. Control of phytoplankton biomass by dilution and mixed layer depth in the western Weddell-Scotia Confluence. *Marine Ecology Process Series*. 366: 15-29.

HOLM-HANSEN, O., MITCHELL, B. G., HEWES, C. D. & KARL, D. M. 1989. Phytoplankton blooms in the vicinity of Palmer Station, Antarctica. *Polar Biology*. 10:49-57.

HOLM-HANSEN, O. & MITCHELL, B. G. 1991. Spatial and temporal distribution of phytoplankton and primary production in the western Bransfield Strait region. *Deep Sea Research*. 38: 961-980.

HOLM-HANSEN, O., KAHRU M., HEWES, C. D., KAWAGUCHI, S., KAMEDA, T., SUSHIN, V. A., KRASOVSKI, I., PRIDDLE, J., KORB, R., HEWITT, R. P. & MITCHELL, B. G. 2004. Temporal and spatial distribution of chlorophyll-*a* in surface waters of Scotia Sea as determined by both shipboard measurements and satellite data. *Deep Sea Research II*. 51: 1323-1331.

JACOBS, S. S. & COMISO, J. C. 1989. Sea ice and oceanic processes on the Ross Sea Continental Shelf . *Journal of Geophysycal Research*. (C12): 195-211.

KANG, S-H., KANG, J-S., LEE, S., CHUNG, K. H., KIM, D. & PARK, M. G. 2001. Antarctic phytoplankton assemblages in the marginal ice zone of the northwestern Weddell Sea. *Journal of Plankton Research*. 23(4): 333-352.

LANCELOT, C., MATHOT, S., VETH, C. & DE BAAR, H. 1993. Factors controlling phytoplankton ice-edge blooms in the marginal ice-zone of the northwestern Weddell Sea during sea ice retreat 1988: Field observations and mathematical modelling. *Polar Biology*. 13(06): 377-387.

LÖSCHER, B. M., DE BAAR, H. J. W., DE JONG, J. T. M., VETH, C. & DEHAIRS, F. 1997. The distribution of Fe in the Antarctic Circumpolar Current. *Deep-Sea Research II*. 44: 143-187.

MARRARI, M., HU, C. & DALY, K. 2006. Validation of SeaWiFS chlorophyll *a* concentrations in the Southern Ocean: A revisit. *Science Direct*. 105: 367-375.

MARRARI, M., DALY, K. L. & HU, C. 2008. Spatial and temporal variability of SeaWiFS chlorophyll a distributions west of Antarctic Peninsula: Implications for krill production. *Deep-Sea Research II*. 55: 377-392.

MARTIN, J. H., GORDON, R. M. & FITZWATER, S. E. 1991. The case for iron. *Limnology and Oceanography*. 36: 1793-1802.

MENDES, C. R., CATAXANA, P. & BROTAS, V. 2007. HPLC determination of phytoplankton and microphytobenthos pigments: comparing resolution and sensitivity of a C_{18} and a C_8 method. *Liminology and Oceanography: Methods*. 5: 362-370.

MITCHELL, B. G. & HOLM-HANSEN, O. 1991. Bio-optical properties of Antarctic Peninsula waters: differentiation from temperate ocean models. *Deep-Sea Research*. 38: 1009-1028.

MITCHELL, B. G., BRODY, E. A., HOLM-HANSEN, O., MCCLAIN, C., BISHOP, J. 1991. Light limitation of phytoplankton biomass and macronutrient utilization in the Southern Ocean. *Limnology and Oceanography*. 36 (8): 1662-1677.

MOLINE, M. A. 1998. Photoadaptive response during the development of a coastal Antarctic diatom bloom and relationship to water column stability. *Liminology and Oceanography*. 43: 146-153.

MONTES-HUGO, M., DONEY, S. C., DUCKLOW, H. W., FRASER, W., MARTINSON, D., STAMMERJHN, S. E. & SCHOFIELD, O. 2009. Recent Changes in Phytoplankton Communities Associated with Rapid Regional

Climate Change Along the Western Antarctic Peninsula. *Science*. 323: 1470-1473.

PIATKOWSKI, U. 1989. Macroplankton communities in Antarctic surface waters: spatial changes related to hydrography. *Marine Ecology Progress Series*. 55: 251-259.

SCHOLDLOK, M. P., HELLMER, H. H., ROHARDT, G. & FAHRBACH, E. 2006. Weddell Sea iceberg drift: Five years of observations. *Journal of Geophysical Research*. 111: C06018.

SCHWARZ, J. N. & SCHODLOK, M. P. 2009. Impact of drifting icebergs on surface phytoplankton biomass in the Southern Ocean: Ocean colour remote sensing and *in situ* iceberg tracking. *Deep-Sea Research I*. 56: 1727-1741.

SEDWICK, P. N. & DiTULLIO, G. R. 1997. Regulation of algal blooms in Antarctic shelf waters by the release of iron from melting sea ice. *Geophysical Research Letters*. 24: 2515-2518.

SEDWICK, P. N., DiTULLIO, G. R. & MACKEY, D. J. 2000. Iron and manganese in the Ross Sea, Antarctica: Seasonal iron limitation in Antarctic shelf waters. *Journal of Geophysical Research*. 105: 11321-11336.

SIMÕES, J. C. 2004. Glossário da língua portuguesa da neve, do gelo e termos correlatos. *Pesquisa Antártica Brasileira*. ISSN 0103-4049. 4: 119-154.

SMITH JR., W. O. & NELSON, D. M. 1990. Phytoplankton growth and new production in the Weddell Sea marginal ice zone in the austral spring and autumn. *Limonology and Oceanography*. 35(4): 809-821.

SMITH JR, W. O., ROBISON, B. H., HELLY, J. J., KAUFMAN, R. S., RUHL, H. A., SHAW, T. J., TWIMING, B. S. & VERNET, M. 2007. Free-Drifting Icebergs:

Hot Spots of Chemical and Biological Enrichment in the Weddell Sea. *Science*. 317: 478-482.

SMITH JR, W. O. & COMISO, J. C. 2008. Influence of sea ice on primary production in the Southern Ocean: A satellite perspective. *Journal of Geophysical Research*. 113(C05S93): 10.1029/2007JC004251.

SONE, T., FUKUI, K., STRELIN, J. A., TORIELLI, C. A. & MORI, J. 2007. Glacier lake outburst flood on James Ross Island, Antarctic Peninsula region. *Polish Polar Research*. 28(1): 3-12.

SPREEN, G., L. KALESCHKE, & G. HEYGSTER. 2008. Sea ice remote sensing using AMSR-E 89 GHz channels, *Journal of Geophysical Research*. doi:10.1029/2005JC003384.

VERNET, M., MARTINSON, D., IANNUZZI, R., STAMMERJOHN, S., KOZLOWSKI, W., SINES, K., SMITH, R. & GARIBOTTI, I. 2008. Primary production within the sea-ice zone west of Antarctic Peninsula: I-Sea ice, summer mixed layer, and irradiance. *Deep Sea Research II*. 55: 20068-2085.

ZAPATA, M., RODRÍGUEZ, F. & GARRIDO, J. L. 2000. Separation of chlorophylls and carotenoids from marine phytoplankton: a new HPLC method using a reserved phase C_8 column and pyridine-containing mobile phases. *Marine Ecology Progress Series*. 195: 29-45.

VIII) APÊNDICES

Apêndice 1. **MANUSCRITO: formatado para o periódico Deep Sea Research Part I.**

Environmental conditions during phytoplankton blooms in the vicinities of the James Ross Island, Antarctic Peninsula

Amália M. S. Detoni[a*]

Carlos A. E. Garcia[a]

Virginia M. T. Garcia[b]

Mauricio M. Mata[a]

[a]*Laboratory of Climate and Oceans Studies*

[b]*Laboratory of Phytoplankton and Marine Microorganisms*

Institute of Oceanography

Federal University of Rio Grande, Av. Italia, km 8, Rio Grande, RS, 96201-900, Brazil,

e-mail: amaliadetoni@gmail.com, dfsgar@furg.br, docvmtg@furg.br, mauricio.mata@furg.br

[*]Corresponding author: Tel. +55 53 32336617, Fax +55 53 32336887, e-mail: amaliadetoni@gmail.com

Abstract

In surrounding waters of James Ross Island (JRI), high chlorophyll-a concentration (Chla) has been detected by ocean color imagery, associated with freshwater streams from JRI glaciers, which contribute with water column stabilization and micronutrient input. In addition, the region is influenced by retreating nutrient-rich sea ice shelf from Weddell Sea in spring and summer, factors that probably fuel phytoplankton primary productivity. However, little is known about variability of phytoplankton blooms on the eastern side of the Antarctic Peninsula, particularly associated with JRI. In this work, the relationship between chlorophyll concentrations (Chla), sea ice and cloud cover in the region has been evaluated by remote sensing time-series analysis (2002–2009). In general, sea ice extent was associated with relatively low average Chla, but high cloud cover also contributed to low summer Chla in some occasions. Samplings have also been conducted in the region in order to characterize and understand the dynamics of phytoplankton biomass associated with the environmental conditions near JRI. Physical, optical, and biogeochemical properties were measured in two cruises carried out during 2008 (1–3 March) and 2009 (17–20 February). A surface water patch of high Chla was first detected using ocean color imagery and subsequently confirmed with *in situ* measurements, where higher phytoplankton biomass was observed in 2009 (around 6 $mg \cdot m^{-3}$). The patches were associated with shallow upper mixed layer depths (33–50m in 2008 and 23–29m in 2009) and relatively high sea surface temperatures, especially during summer 2009, with minimum temperatures > -0.95°C. Our results support the hypothesis that phytoplankton biomass near JRI may be related to melt of JRI glaciers, providing shallow mixed layer depths, beyond the study area is shielded local from wind from southwest, which help to sustain the stratification of water column. A different condition was observed in the Antarctic Sound (channel between Peninsula tip and Joinville Island), where low Chla values were associated with no influence of freshwater streams and a deep mixed layer in both summers. Those conditions prevented phytoplankton biomass accumulation in the photic layer in that region. We conclude that the magnitude and spatial changes in phytoplankton biomass in the region are associated with local alterations in the environmental conditions, such as retreat of tidewater glaciers in JRI in conjunction with sea ice shelf retreat and also cloud cover in some occasions.

Keywords: Tidewater glacier, Sea ice, Phytoplankton bloom, Meltwater, Mixed layer depth.

1. Introduction

The Southern Ocean is characterized by macronutrients availability that would support a high primary productivity; however, in general, chlorophyll-a and primary productivity rates are typical of oligotrophic to mesotrophic ocean environments (Fiala *et al*., 1998; Garibotti *et al*., 2005). Where large phytoplankton blooms do occur during austral spring and summer, they are mainly associated with ice edges, polynyas, islands, continental shelves and oceanographic frontal regions (Smith and Nelson, 1990; Garibotti *et al*., 2003; Arrigo and van Dijken, 2004).

Phytoplankton growth in the Southern Ocean is controlled by many factors, such as: light availability, ice cover, winds, iron availability and zooplankton grazing (Holm-Hansen *et al*., 1989, Mitchell *et al*., 1991, Constable and Nicol, 2003, Marrari *et al*., 2008). However, the degree to which the physical, chemical and biological factors could limit the phytoplankton growth is not completely understood and their relative importance can vary with location, season and local meteorological conditions (Lancelot *et al*., 1993). Understanding the large-scale relationships between phytoplankton growth/biomass and physical forcing in the Southern Ocean is essential for a complete knowledge of the mechanisms controlling the food webs and biogeochemical cycles in the Antarctica (Smith and Comiso, 2008).

Previous theoretical and empirical models suggested that water column stability, grazing and/or resource limitation are the main factors that govern the dynamics of phytoplankton blooms in Polar Regions (Michell and Holm-Hansen, 1991). While these studies have advanced the knowledge of mechanisms that control phytoplankton dynamics, they also point to the need of studies with better space resolution of biological and physical processes (Michell and Holm-Hansen, 1991).

Sea ice dynamics appear to have a great influence over the coastal phytoplankton at Polar Regions (Smith *et al*., 1998; Garibotti *et al*., 2003; Arrigo *et al*., 2008). Sea ice melting acts particularly as source of nutrients (including iron) (Sedwick and DiTullio, 1997) and contributes to stratification of surface waters. Sea ice mau accumulate iron from atmospheric deposition of mineral dust (Edwards and Sedwick, 2001) and may also incorporate iron from sedimentary sources when forming in coastal/shelf regions (Sedwick *et al.*, 2000, Fitzwater *et al.*, 2000, Grotti *et al.*, 2005). Low salinity meltwater produces low-density surface layers that reduces vertical mixing and shallows the mixed layer depth, providing excellent conditions for high primary productivity (Boyd, 2002, Garibotti *et al*., 2003, Marrari *et al*., 2008). The variability of the phytoplankton community as reported by Garibotti *et al.* (2003) was related to differences in the local environmental parameters and reflected the different temporal stages of the seasonal succession of algae assemblages, as a consequence of the progressive retreat of the sea ice from north to south along the western Antarctic Peninsula.

Changes in sea ice cover dynamics due to global warming (earlier retraction of the sea ice) may not affect directly Antarctic phytoplankton composition but induce some instability on their seasonal dynamics with impacts on the food web (Garibotti *et al.*, 2003). However, Montes-Hugo *et al.* (2009) have demonstrated that in the western side of the Antarctic Peninsula two different trends in chlorophyll-a concentration can be detected in a latitudinal gradient. An increasing trend in the southern part was accompanied by shifts in the community composition, with a greater fraction of diatoms and large cells, associated with decrease in summer sea ice extent in areas that were previously sea ice covered most of the year.

The study area, northeast of the Antarctic Peninsula (see Fig. 1), under Weddell Sea influence, is usually covered by sea ice, with a marginal ice zone of high phytoplankton biomass and productivity (Park *et al*., 1999). The sampling area is close to James Ross Island (JRI), which presents almost 80% of the Island area occupied by glaciers (Sone *et al*., 2007). The island receives abundant precipitation and melts significantly in the summer months, drained by fast glaciers (Hawes and Brazier, 1991; Sone *et al*., 2007). The glacier lakes flood outburst was observed during 2004–2005 austral summer, which may be result of the recent rapid climate warming in this region (Sone *et al*., 2009). Thus, meltwater derived from those glaciers, and the abundance of icebergs in the region, exerts an important influence on the coastal marine ecosystem by changing the upper thermohaline properties of seawater (Pisarevskava and Popov, 1991).

In this article, we report environmental conditions in the vicinities of James Ross Island, where high values of chlorophyll concentration are recurrently detected by satellite ocean color images. However, it is known that in the Southern Ocean limitations such as clouds and/or sea ice cover hinder the understanding of phytoplankton distributions and inter-annual changes from ocean color images. For this reason, were estimated the clouds covered areas in respect of open waters areas and sea ice areas, in order to investigate inter-annual changes in the primary productivity areas in these waters by ocean color images.

The hydrographic and biological conditions of the northeastern of Antarctic Peninsula are dominated by meteorology (wind and temperature) via its control over sea ice dynamics (e.g., formation, advection, and melt) and upper ocean stratification. Stations located near JRI are sheltered by winds, and receives input of melting from next continents. Thus, samplings were conducted during two successive years in the region, where physical, optical, and biogeochemical properties were measured to characterize the environmental conditions associated with the phytoplankton blooms.

Here we investigate the inter-annual changes in the phytoplankton blooms that form in summer in the northeastern of Antarctic Peninsula by remote sensing, and how the blooms phytoplankton found near of JRI had behaved associated with environmental conditions observed during two consecutive summers.

2. Methods

2.1. Study area and cruises

The study area comprised coastal waters east of the tip of the Antarctic Peninsula, adjacent deep waters in the northwestern Weddell Sea and the marginal ice zone (Fig. 1A). The cruises were conducted in 2008 (1–3 March) and 2009 (17–20 February) as part of the project “Southern Ocean Studies for Understanding Global Climate Issues (SOS-CLIMATE)”, a Brazilian contribution to the IV International Polar Year.

The sampling area was close to James Ross Island (JRI) (Fig. 1B). The number of CTD stations occupied during the SOS-I (2008) and SOS-II (2009) cruises were 20 and 12, respectively (Fig. 1C and D).

2.2. Oceanographic Data

Vertical profiles of temperature, salinity, fluorescence and beam-attenuation, (*c*) at 660nm, were taken with a Sea-Bird CTD/Carrousel 911+ system®. We use temperature, salinity, pressure measurements during the CTD downcast profiles, while stimulated fluorescence, beam-attenuation, and dissolved oxygen data were taken from CTD upcast profiles, since seawater was sampled during the upcast profiles, using 5L Niskin bottles. In this way, we tried a more accurate and precise relationship between chlorophyll-*a* concentrations and optical properties measured by attached sensors to the CTD/Carrousel system.

Corrections for instrument calibration, fouling, and drift were made by referencing all attenuation data. Was found a constant value of beam attenuation in the deeper station to each cruise measured at depths of ~2100–2200m, where are not appearing phytoplankton cells anymore. These beam attenuation values, corresponding to each cruise, were subtracted of all data set of beam attenuation, considering an offset into the data set. SOS-I presents an offset of $0.04 m^{-1}$, and SOS-II an offset of $0.17 m^{-1}$. This procedure was applied in order to all values of beam attenuation reported here refer to particulate attenuation at 660nm.

In situ stimulated fluorescence was used as a proxy of phytoplankton biomass, based on a strong linear relationship between fluorescence and chlorophyll concentrations ($r = 0.86$, $n= 32$, $p< 0.001$).

2.3. Measurement of phytoplankton pigments

Seawater samples of 0.5-1 L were filtered onto Whatman 25mm GF/F filters and the filters were immediately stored in liquid nitrogen. Photosynthetic pigments were extracted with 2mL of 95% cold-buffered methanol (2% ammonium acetate) for 30min at –20°C, in the dark. The samples were sonicated (Bransonic, model 1210) and centrifuged. Extracts were filtered (Fluoropore PTFE filter membranes, 0.2μm pore size) and immediately analyzed in the HPLC. The HPLC method, based on a monomeric C8 column and a pyridine-containing mobile phase, followed Zapata *et al.* (2000) adapted by Mendes *et al.* (2007).

Chlorophyll-a concentration was calculated from the signal in the photodiode array detector and HPLC system was calibrated with a Sigma commercial standard.

2.4. Mixed Layer Depth

Hewes *et al.* (2008) determined the bottom of the upper mixed layer for Elephant Island and South Shetland Islands regions as the depth at which potential density differed by 0.05 kg·m^{-3} from the mean potential density measured between 5 and 10m depth, where it seems that the increased upper mixed layer (UML) depth is the factor controlling the biomass in those waters. Thus, the UML depth in this study was calculated according to Hewes *et al.* (2008), however an adjustment was necessary because the potential density differential found in our data set along of the water column was 0.02 kg·m^{-3}, in the other words, the maximum value of the difference between the mean potential density, found between 5 and 10m depth, and of potential density along the potential density profile into water column.

2.5. Satellites data

Chlorophyll-a (Chla) concentration data were derived from monthly composites of MODIS-Aqua satellite images. The Level 3 (L3) (Standard Mapped Image) SMI images were obtained from http://oceancolor.gsfc.nasa.gov at 4 km resolution.

Daily images of sea ice concentration were used for calculating mean monthly images of the study area. The selected period was October to March for years 2002 to 2009; the data were collected from AMSR-E sensor, with a spatial resolution of approximately 6x4 km at 89 Ghz. The Artist Sea Ice (ASI) algorithm was applied, which uses an empirical model to retrieve the ice concentration between 0% and 100% (Spreen *et al*., 2008). Daily maps of hemispherical (6.25km grid) sea ice concentration (ASI algorithm) are operationally provided by the Institute of Environment Physics, University of Bremen (*www.iup.physik.uni-bremen.de*).

The mean monthly areas of sea ice cover, exposed ocean and open water covered by clouds within the study area during analyzed months (October to March) were determined using imagery from both the AMSR-E and MODIS-Aqua. The selected area was latitudes 64.5°S to 63.2°S and longitudes 57.7°W to 54°W, hence focusing only on the region northeast of JRI. For each month, open water pixels were first identified by ASI algorithm where sea-ice concentration of pixel was ≤ 15%, which is in general defined as the ice edge (Marrari *et al*., 2008, Spreen *et al*., 2008). The sea ice area was determined from pixels that contained > 15% of sea ice concentration. MODIS-Aqua image for the same month was then compared to the AMSR-E image and MODIS-Aqua pixels over open water (as defined above) that was masked (without data) as being either cloud or ice covered was assumed to be covered by clouds.

The spatial resolution of AMRS-E pixel was determined by the total pixel area defined from spatial resolution of MODIS-Aqua image (4x4 km), and then was divided by the total number of AMRS-E pixels.

3. Results and Discussion

3.1. Satellite data of Chlorophyll-a (Chla) and sea ice concentration

The mean monthly Chla concentration between October and March for seven austral summers in the study area (Fig. 2) shows peaks in December 2004 and February (austral summer). The interannual variability in Chla is mostly associated with sea ice cover; however, missing values due to cloud cover can partly account for the observed variability. Phytoplankton growth rates in early stages of a bloom are strongly controlled by light availability; therefore, it is important to evaluate interannual differences in cloud cover, which can reduce incident irradiance by more than 50%. Moreover, this information helps understanding differences observed in sensor MODIS-Aqua chlorophyll time series.

The fraction of each component (ocean, sea-ice, clouds) are shown at Fig. 3 for the study area from 2002 to 2009, during spring and summer, based on data from the satellite sensors. Sea ice extent was particularly high in 2002–03, 2003–04 and again in 2007–08, associated with relatively low average Chla (Fig. 2). In 2002–03, particularly, cloud cover (around 35%) may have also contributed to low Chla in summer. However, the low Chla in 2006–07was not associated with either cloud or sea ice cover. These low Chla may be associated with either physical processes such as deepening of the upper mixed layer or biological processes, such as grazing pressure. On the other hand, the nearly disappearance of sea-ice during 2008–09 can explain the higher chlorophyll-a concentrations estimated by the sensor MODIS-Aqua.

The fraction of open water covered by clouds exhibited a varying seasonal pattern between observed years. Open waters during the October months were rarely exposed to sunny skies. A maximum in sea ice cover is also found in October at this region (Arrigo and van Dijken, 2004), which is partly due to reflection associated with cloudiness this time of year. In our data, this was also associated with extremely small amounts of open water in the study region during October. The amount of exposed open water increased mainly from December each year, with the maximum of about 85% of ice free ocean area in February 2009 (Fig. 3).

In the period October to March, the sea ice showed strong interannual variability, ranging from 97% in October and 11% in March in 2002–2003 to over 6% in October and 15% in March 2008–2009 (Fig. 3).

A physical connection may exist between the amount of open water and the presence of sea ice, which could be the result of enhanced solar radiation during the austral summer when cloud abundance is low. This allows increased radiative heating of the sea surface and enhanced sea ice melt, thus controlling the sea ice dynamics and exposed ocean area, influencing the dynamics of phytoplankton growth and primary productivity of the region (Jacobs and Comiso, 1989, Arrigo and van Dijken, 2004). For instance, it has been shown that alongshore phytoplankton distribution in the western Antarctic Peninsula has been adjusting to the ongoing long-term sea ice decline and spatial modifications of other physical climate factors (Montes-Hugo *et al*., 2009). The authors have shown that in the southern portion of the shelf, remotely sensed chlorophyll has undergone a remarkable increase from 1978–1986 (CZCS) to 1998–2006 (SeaWIFS) that can be attributed mainly to rapid regional climate change. They associated this trend with a substantial decrease in sea ice extent, cloud cover and wind intensity. The data in our study suggests that cloud cover and especially sea ice extent were the main factors driving the variability in Chla. However, wind-driven changes in the mixed layer depth may have influenced the low Chla values observed in some years, such as 2006–2007.

The spatial and temporal patterns in Chla suggest that biomass accumulations normally appear in early February near JRI, progressively moving south and later, as the season progresses and sea ice melts, phytoplankton blooms develop further south, near 64-65ºS . Holm-Hansen *et al.* (2004) observed that the ice-edge bloom northeast of the Antarctic Peninsula moved progressively southward and intensified from December 1999 through February 2000 and reaching the highest bloom (> $4 mg \cdot m^{-3}$) in February 2000, in contrast, the rich bloom to the northeast of South Georgia, north of the study area, is highest in December and decline progressively through January and February.

Based on analysis of multi-temporal satellite image data for 1988–2001 period, Rau *et al.* (2004) showed that the recession of glaciers on JRI increased at a rate $3.79 km^2 \cdot y^{-1}$. They state that the observed glacial variations in the northeastern Antarctic Peninsula are interpreted as direct consequences of the rapidly changing climatic conditions in the region, which are affecting accumulation and ablation. In contrast, observations from the northwest of the Antarctic Peninsula, which is presumed to be in the natural range of frontal fluctuations of tidewater glaciers, suggest relative dynamic stability of the glacial systems in this sector (Rau *et al*., 2004).

Monthly images of MODIS-Aqua sensor from summers 2007/2008 and 2008/2009 (January and February 2008 and 2009) are presented at Fig. 4, associated with sea ice concentration data, which is marked in black in the images. Sea ice concentration data of both cruises SOS-I and SOS-II shows that ice free areas in summer 2008/2009 (January and February 2009) is greater than summer 2007/2008. The whole sea ice area found in October both 2007 and 2008, 17.4% were melted in February 2008, whereas, 87.7% were melted in February 2009. The increase in ice-free summer days translates into more favorable conditions in the upper mixed layer (UML), providing increased light levels, for phytoplankton growth, as seen in ocean color chlorophyll images for both years (Fig.4). In the western region, it has been suggested that the sea ice extent and phytoplankton dynamics changes are expected to enhance photosynthesis and chlorophyll-a accumulation due to lower light limitation and that this may be happening in other areas around the Antarctic Peninsula (Rasmus *et al*., 2004; Montes-Hugo *et al*., 2009). Few studies have provided information on phytoplankton dynamics in the northeastern Antarctic Peninsula, but our results suggest that probably the changing patterns in phytoplankton biomass and composition observed in the western side (Montes-Hugo *et al*., 2009) may be occurring also in the vicinities of the JRI.

3.2. Oceanographic properties in the study region

The T/S diagrams for both cruises in the JRI region can be shown at figure 5, where shows three different kinds of surface waters, the Weddell Sea Shelf Waters (WSSW) is detached in yellow, Meltwater, with lower salinities, in blue, and Confined Water, with higher salinities, in red. WSSW is an important source of nutrient in the region, fertilizing surface waters of the eastern shelf of the Antarctic Peninsula with both macro and micronutrients, including iron (Sañudo-Wilhelmy *et al*., 2002). This surface water source is cold (-1.3 to 0.7 ºC) and saline (> 34) (Piatkowski, 1989; Gordon *et al*., 2000) as observed in T/S values during our two cruises. This water was mainly observed in surface waters, which were represented here as waters within the upper mixed layer (see Fig. 5). The WSSW flows in a northwesterly direction and enters the Bransfield Strait through the Antarctic Sound (AS) and around the tip of the Antarctic Peninsula, as shown by Piatkowski (1989).

Surface layers in our study region, associated with waters derived from horizontal mixing with fresh meltwater which is originated from JRI glaciers, with temperatures between -0.7 to -1.2°C and salinity lower than 34.27. This surface water can be seen in the SOS-I and SOS-II T/S diagram as blue dots (Fig. 5).

In the AS there is a channel deep enough to provide a pathway for shelf water (Gordon *et al*., 2000). We observed a confined water, here considering just until upper mixed layer depth which about 100m, that was likely advected from WSSW and remained within this channel between the Bransfield Strait and Weddell Sea. This water mass is warmer and saline (Fig. 5), with salinities between 34.35 to 34.4 in both cruises and temperatures between the -0.9 to -0.6°C, as seen in red dots. This water was seen at stations R118, R119 and R120 (SOS-I), and at stations R209, R210 and R211 (SOS-II). Furthermore, those sites presented deeper UML depth, over 100m (Fig. 6 C and F) likely caused by stronger turbulence within the AS. Hewes *et al.* (2008) showed that given the nutrient- and trace metal- replete conditions at salinities > 34, it seems likely, that the increased UML depth is the factor controlling phytoplankton biomass in western Antarctic Peninsula waters.

Surface distribution of temperature, salinity and depth of the UML can be shown at Fig. 6. Higher temperatures were observed in sea surface during SOS II (-0.93°C to -0.43°C) than in SOS I (-1.19°C to -0.62°C), (Fig. 6 A and D). Thermal characteristics of surface waters in the Southern Ocean are dominated by exchange with the atmosphere, sea-ice dynamics and interaction with deeper waters (Smith and Klinck, 2002). The relatively high sea surface temperature, when enriched with iron, can benefit phytoplankton through the enhanced shoaling of the UML.

This increase of sea surface temperature may had contributed with early process of melting sea ice observed in summer 2008/2009, and can also release dissolved trace metal concentration, mainly iron, into surface waters, suggesting that both the availability of light, through a lower UML depth, and iron, are fueling the phytoplankton blooms. Considering future studies, such environmental changes will clearly impact the primary productivity of the system by altering nutrients inputs from coastal and upwelling regions (Hewes *et al*., 2008).

Surface salinities were lower in SOS-II (Fig. 6B and E), likely due to a stronger presence of fresher water in 2009. This decrease was inversely related with both Chla and beam attenuation (see Fig. 7). For instance, close to JRI (Stn R113 to R115) salinity was low (34.15 to 34.25) indicating a region of continental ice melt.

Surface distributions of biological and optical parameters in both years at the JRI region can be presented at Fig 7. The distribution of fluorescence intensity and beam attenuation coefficient (*c*) followed very closely the Chla distribution, with higher values close to JRI, particularly at the second cruise, indicating that phytoplankton significantly contributed to light attenuation. Chla at surface varied from 0.25 to $4.53 mg \cdot m^{-3}$ in SOS-I and 0.36 to $7.61 mg \cdot m^{-3}$ in SOS-II. Chla, fluorescence and beam attenuation coefficient (*c*) (Fig. 7) presented the highest values at those stations, indicating a positive influence of meltwater on phytoplankton biomass accumulation. The stations near JRI showed high surface values of *c*, ranging from 0.15 to $0.39 m^{-1}$ in SOS-I cruise. In the SOS-II cruise, highest values of *c*, greater than $0.62 m^{-1}$, were observed over the bloom (maximum Chla in the UML 8.84mg·m^{-3}) in the vicinities of JRI. However, high attenuation values were also observed in the AS in SOS-II, but not associated with phytoplankton, probability associated with suspended material.

An inverse relationship between Chla and salinity in the UML, for both cruises, can be seen at Fig. 8. Hewes *et al.* (2009) found a unimodal pattern of Chla concentration across salinity gradients in waters surrounding the South Shetland Island (western Antarctic Peninsula). They state that phytoplankton biomass is mainly controlled by UML depth at higher salinities and by iron at lower salinities, with optimal conditions at intermediate values around 34. Salinity was also associated with phytoplankton size classes, where small cells dominated the coastal bloom biomass at mid salinity (~34) waters, while large cells composed substantial fractions of low Chla populations and lower salinities in the Antarctic Circumpolar Current. In our study area, we found that phytoplankton biomass was maximal where WSSW and continental melting waters interact to produce a shallow UML and likely contribute to elevated nutrients and trace metals in the vicinities of JRI region. Given the different conditions found within the study area in both years, the discharge of continental melting water from JRI can especially influence the observed phytoplankton blooms, through stratification and thus generating a shallow mixed layer.

In summary, in the study region fresher glacier waters (Fig. 6B and E) were associated with high Chla (Fig. 7A and D) and relatively shallow mixing layer conditions (Fig. 6C and F). Those conditions are observed at the bloom patches (Chla>1.62mg·m^{-3} in SOS-I and Chla>3.2mg·m^{-3} in SOS-II), near JRI, followed by high fluorescence and high *c*. This surface core was associated with two different water masses at the mixing layer: continental, cold, low-salinity meltwater from JRI, and

WSSW, which is probably a source of iron. The highest Chla occurred where the UML depth shoaled (29–33m in SOS-I and 18–30m in SOS-II), combined with lower salinities, providing an environment conducive of enhanced phytoplankton primary production.

3.3. Relationships between biological and optical data

The relationships between fluorescence intensity and Chla (0–150m), which were very good in both cruises ($r = 0.88$, $n = 63$, $p<0.001$ and $r = 0.91$, $n = 42$, $p<0.001$, for SOS-I and SOS-II, respectively), can be seen at Fig. 9A. Based on those relationships, values of fluorescence intensity were considered to Chla in order to compare with attenuation (*c*) in both cruises. The data set was then separated into stations in the vicinities of JRI (black dots in the graphics Fig. 9B and 9C) and data for the remaining stations (gray dots in the graphics Fig. 9B and 9C), in both cruises.

Data set distribution of SOS-I are represent at Fig. 9B, and the Fig. 9C represents the SOS-II. The relationship was high for data were high near JRI (Fig. 9B and 9C) both in SOS-I and SOS-II ($r = 0.96$ and $r = 0.87$ respectively), indicating that phytoplankton was the major component contributing to light attenuation within the high Chla patches. However, at stations far from the phytoplankton bloom and within the AS showed a very poor relationship in SOS-II (Fig. 9C), indicating that other components in the water column were more important for light attenuation. ($r = 0.94$ for stations in SOS-I, $r = -0.40$ for stations in SOS-II). Probably, those stations associated with lower Chla had a relatively high content of particulate material (both organic and inorganic particulates), which must have significantly contributed to light attenuation. Michell and Holm-Hansen (1991) found a layer of strongly attenuating water and low

Chla near a shoal in the western Antarctic Peninsula, which they attributed to resuspension of bottom sediments. However, a strong relationship was shown in SOS-I, indicating that particulate material is associated with phytoplankton cells in this cruise, although low Chla concentrations (~0.55mg·m^{-3}) were found in stations located in the AS. This may be caused by adaptation to low light levels, where the proportion of pigment per cell is increased (Mitchell, 1992), thus a diminishing number of cells per unit of chlorophyll may account for a relative reduction in beam attenuation (Loisel & Morel, 1998).

In summary, phytoplankton relates very well to water column light attenuation in areas with high Chla at surface, near JRI (Chla>1.62mg·m^{-3} in SOS-I and Chla>3.2 mg·m^{-3} in SOS-II), although the relationship was slightly different between both years. In sites with lower Chla at surface (<1.4mg·m^{-3} in SOS-I and <2.8mg·m^{-3} in SOS-II), phytoplankton was either related to beam attenuation under low light conditions (SOS-I) or showed no relationship, indicating the influence of other particular material, such as sediments and/or particular organic matter.

4. Conclusion

In the surroundings of James Ross Island, as summer approaches, seawater becomes ice-free and the glaciers rapidly start melting. The glacier flow into oceanic waters change the stability of the upper layer, an important physical mechanism for maintaining phytoplankton in the photic layer, and also provides iron biologically available for phytoplankton growth. Iron derived from melting sea-ice and snow can also provide more micronutrient to the upper oceanic waters, which enhances the phytoplankton blooming in the vicinities of the JRI area. The high Chla found in the study area were associated with relatively low salinities, thus indicating melting waters, while low Chla were found in mixed waters, mainly in the Antarctic Sound. High beam attenuation and low fluorescence at that region and other sites far from the bloom indicate that different hydrodynamic processes such as a deep UML depth, limited phytoplankton growth.

The phytoplankton blooms at eastern Antarctic Peninsula tip are influenced by freshwater from glaciers, when summer primary production is associated with freshwater runoff onto surface waters, strengthening stratification and decreasing the UML depth.

Our study showed changes in the intensity of phytoplankton blooms sampled during two consecutive years. These changes likely act as response of local alterations in the environment, which, probably, are caused by both retreat of tidewater glaciers at JRI and increase in ice-free summer days mainly during February 2009.

Acknowledgements

This project is part of GOAL (Group of High Latitude Oceanography) and was support by the funding resources of CNPq (Brazilian National Council on Research and Development) and MMA (Ministry of Environment) to the Brazilian Antarctic Program (PROANTAR). The authors would like to thank the crew of the Brazilian Navy research ship "*Ary Rongel*" for their assistance and for contributing to the success of the cruises. We are very grateful to Rafael Mendes for HPLC analysis. This research is part of a master dissertation, with fellowship to AMSD from CAPES (Brazilian Coordination Agency for Improvement of High Level Personnel).

References

Arrigo, K. R. and van Dijken, G. L., 2004. Annual changes in sea-ice, chlorophyll *a*, and primary production in the Ross Sea, Antarctica. Deep-Sea Research Part II**.** 51, 117-138.

Arrigo, K. R., Dijken, G. L. and Bushinsky, S., 2008. Primary production in the Southern Ocean, 1997 - 2006. Journal of Geophysical Research, 113(C08004): 1 - 27.

Boyd, P. W. 2002. Environmental Factors Controlling Phytoplankton Processes in the Southern Ocean. Journal Phycology: An international Journal of Algal Research. 38, 844-861.

Constable, A. J. and Nicol, S., 2003. Southern Ocean productivity in relation to spatial and temporal variation in the physical environment. Journal of Geophysical Research. 108 (C4): 8079.

Fiala, M., Kopczynska, E. E., Jeandel, C., Oriol, L. and Vetion, G., 1998. Seasonal and interannual variability of size-fractioned phytoplankton biomass and community structure at station Kerfix, off the Kerguelen Island, Antarctica. Journal of Plankton Research. 20(07), 1341-1356.

Fitzwater, S. E., Johnson, K. S., Gordon, R. M., Coale, K. H. and Jr Smith, W. O., 2000. Trace metal concentrations in the Ross Sea and their relationship with nutrients and phytoplankton growth. Deep-Sea Research II. 47, 3159-3179.

Garibotti, I. A., Vernet, M., Ferrario, M. E., Smith, R. C., Ross, R. M. and Quetin, L. B., 2003. Phytoplankton spatial distribution patterns along the western Antarctic Peninsula (Southern Ocean). Marine Ecology Progress Series. 261, 21-39.

Garibotti, I. A., Vernet, M., Smith, R. C. and Ferrario, M. E., 2005. Interannual variability in the distribution of the phytoplankton standing stock across the seasonal sea-ice zone west of the Antarctic Peninsula. Journal of Plankton Research. 27(8), 825-843.

Gordon, A. L., Mensch, M., Dong, Z., Smethie, W. M. and de Bettencour, J., 2000. Deep and bottom water of the Bransfield Strait eastern and central basins. Journal of Geophysical Research. 105, 11,337-11,346.

Grotti, M., Soggia, F., Ianni, C. and Frache, R., 2005. Trace metals distributions in coastal sea ice of Terra Nova Bay, Ross Sea, Antarctica. Antarctic Science. 17 (2), 289-300.

Hawes, I. and Brazier, P., 1991. Freshwater stream ecosystems of James Ross Island, Antarctica. Antarctic Science. 3, 265–271.

Hewes, C. D., Reiss, C. S., Kahru, M., Miltchell, B. G. and Holm-Hansen, O., 2008. Control of phytoplankton biomass by dilution and mixed layer depth in the western Weddell-Scotia Confluence. Marine Ecology Progress Series. 366, 15-29.

Hewes, C. D., Reiss, C. S. and Holm-Hansen, O., 2009. A quantitative analysis of sources for summertime phytoplankton variability over 18 years in the South Shetland Islands (Antarctica) region. Deep-Sea Research Part I. 56, 1230-1241.

Hewes, C. D., 2009. Cell size of Antarctic phytoplankton as a biogechemical condition. Antarctic Science. Doi:10.1017/S0954102009990125, 1-14.

Holm-Hansen, O., Mitchell, B. G., Hewes, C. D. and Karl, D. M., 1989. Phytoplankton blooms in the vicinity of Palmer Station, Antarctica. Polar Biology. 10:49-57.

Holm-Hansen, O. and Mitchell, B. G., 1991. Spatial and temporal distribution of phytoplankton and primary production in the western Bransfield Strait region. Deep-Sea Research. 38, 961-980.

Holm-Hansen, O., Kahru, M., Hewes, C. D., Kawaguchi, S., Kameda, T., Sushin, V. A., Krasovski, I., Priddle, J., Korb, R., Hewitt, R. P. and Mitchell, B. G., 2004. Temporal and spatial distribution of chlorophyll-a in surface waters of the Scotia Sea as determined by both shipboard measurements and satellite data. Deep-Sea Research Part II. 51, 1323-1331.

Jacobs, S. S. and Comiso, J. C. 1989. Sea ice and oceanic processes on the Ross Sea Continental Shelf . Journal of Geophysical Research. (C12), 195-211.

Lancelot, C., Mathot, S., Veth, C. and Baar, de H., 1993. Factors controlling phytoplankton ice-edge blooms in the marginal ice-zone of the northwestern Weddell Sea during sea ice retreat 1988: Field observations and mathematical modelling. Polar Biology. 13(06), 377-387.

Loisel H. and Morel, A., 1998. Light scattering and chlorophyll concentration in case 1 waters: A reexamination. Limnology and Oceanography. 43(5), 847-858.

Marrari, M., Hu, C. and Daly, K., 2006. Validation of SeaWiFS chlorophyll *a* concentrations in the Southern Ocean: A revisit. Science Direct. 105, 367-375.

Marrari, M., Daly, K. L. and Hu, C., 2008. Spatial and temporal variability of SeaWiFS chlorophyll a distributions west of Antarctic Peninsula: Implications for krill production. Deep-Sea Research II. 55, 377-392.

Mendes, C. R., Cataxana, P. and Brotas, V., 2007. HPLC determination of phytoplankton and microphytobenthos pigments: comparing resolution and sensitivity of a C_{18} and a C_8 method. Limnology and Oceanography: Methods. 5, 362-370.

Mitchell, B. G. and Holm-Hansen, O., 1991. Bio-optical properties of Antarctic Peninsula waters: differentiation from temperate ocean models. Deep-Sea Research. 38, 1009-1028.

Mitchell, B. G., Brody, E. A., Holm-Hansen, O., McClain, C. and Bishop, J., 1991. Light limitation of phytoplankton biomass and macronutrient utilization in the Southern Ocean. Limnology and Oceanography. 36 (8): 1662-1677.

Mitchell, B. G., 1992. Predictive bio-optical relationships for polar oceans and marginal ice zones. Journal of Marine Systems. 3, 91-105.

Montes-Hugo, M., Doney, S. C., Ducklow, H. W., Fraser, W., Martinson, D., Stammerjhn, S. E. and Schofield, O., 2009. Recent Changes in Phytoplankton Communities Associated with Rapid Regional Climate Change Along the Western Antarctic Peninsula. Science. 323, 1470-1473.

Park, M. G., Yang, S. R., Kang, S., Chung, K. H. and Shim, J. H. 1999. Phytoplankton biomass and primary production in the marginal ice zone of the northwestern Weddell Sea during austral summer. Polar Biology. 21, 251-261.

Piatkowski, U. 1989. Macroplankton communities in Antarctic surface waters: spatial changes related to hydrography. Marine Ecology Progress Series. 55, 251-259.

Pisarevskaya, L. G. and Popov, I. K., 1991. Free-drifting icebergs and thermohaline structure. Glaciers-Ocean-Atmosphere Interactions. 208: 447-454.

Rasmus, K. E., Granéli, W. and Wängberg, S. A., 2004. Optical studies in the Southern Ocean. Deep-Sea Research II. 51, 2583-2597.

Rau, F., Mauz, F., De Angelis, H., Jaña, R., Neto, J. A., Skvarca, P., Vogt, S., Saurer, H. and Gossmann, H., 2004. Variations of glaciers frontal positions on the northern Antarctic Peninsula. Annals of Glaciology. 39, 525-530.

Sañudo-Wilhelmy, S. A., Olsen, K. A., Scelfo, J. M., Foster, T. D. and Flegal, A. R., 2002. Trace metal distributions off the Antarctic Peninsula in the Weddell Sea. Marine Chemistry. 77, 157-170.

Sedwick, P. N. and DiTullio, G. R., 1997. Regulation of algal blooms in Antarctic shelf waters by the release of iron from melting sea ice. Geophysical Research Letters. 24, 2515-2518.

Sedwick, P. N., DiTullio, G. R. and Mackey, D. J., 2000. Iron and manganese in the Ross Sea, Antarctica: Seasonal iron limitation in Antarctic shelf waters. Journal of Geophysical Research. 105, 11321-11336.

Smith, R. C., Baker, K. S. and Vernet, M., 1998. Seasonal and interannual variability of phytoplankton biomass west of the Antarctic Peninsula. Journal of Marine Systems. 17, 229-243.

Smith Jr., W. O. and Nelson, D. M., 1990. Phytoplankton growth and new production in the Weddell Sea marginal ice zone in the austral spring and autumn. Limonology and Oceanography. 35(4), 809-821.

Smith Jr, W. O. and Comiso, J. C., 2008. Influence of sea ice on primary production in the Southern Ocean: A satellite perspective. Journal of Geophysical Research. 113(C05S93), 10.1029/2007JC004251.

Sone, T., Fukui, K., Strelin, J. A., Torielli, C. A. and Mori, J., 2007. Glacier lake outburst flood on James Ross Island, Antarctic Peninsula region. Polish Polar Research. 28(01), 3-12.

Spreen, G., Kaleschke, L. and Heygster, G., 2008. Sea ice remote sensing using AMSR-E 89 GHz channels, J. Geophys. Res., doi:10.1029/2005JC003384

von Gyldenfeldt, A. B., Fahrbach, E., García, M. A. and Schröder, M., 2002. Flow variability at the tip of the Antarctic Peninsula. Deep-Sea Research Part II. 49, 4743-4766.

Wright, S. W. and van den Enden, R. L., 2000. Phytoplankton community structure and stocks in the East Antarctic marginal ice zone (BROKE survey, January-March 1996) determined by CHEMTAX analysis of HPLC pigment signatures. Deep-Sea Research II. 47, 2363-2400.

Zapata, M., Rodríguez, F. and Garrido, J. L., 2000. Separation of chlorophylls and carotenoids from marine phytoplankton: a new HPLC method using a reserved phase C_8 column and pyridine-containing mobile phases. Marine Ecology Progress Series. 195, 29-45.

Figure Captions

Figure 1. (A) Map of Antarctica showing the Antarctic Peninsula tip. (B) Map of the Antarctic Peninsula showing the location of the study area and other geographic references. (C) Locations of the CTD stations during 1–3 March 2008. (D) Locations of the CTD stations during 17–20 February 2009.

Figure 2. Time evolution of monthly mean chlorophyll-*a* concentration, estimated by MODIS-Aqua sensor, during October to March (summer austral) for years 2002–2009 period, in the vicinities of the James Ross Island, eastern of Antarctic Peninsula (64.5°S – 63.2°S, 57.7°W – 54°W).

Figure 3. Relative fractions of open water area, open water covered by clouds and sea ice cover area from October to March, years 2002–2009.

Figure 4. MODIS-Aqua imagery of monthly mean chlorophyll-a concentration (pallet), showing also the mean location of sea ice cover (black pixels). (A, B) SOS-I Cruise in January–February 2008. (C, D) SOS-II Cruise in January – February 2009.

Figure 5. Potential temperature and salinity diagram (T-S) for the study area during (A) SOS-I Cruise 2008 and (B) SOS-II Cruise 2009 in the vicinities of James Ross Island. The colored dots represent waters within the upper mixed layer. The Meltwater (blue) was present at stations #118, #119 e #120 (SOS-I) and #210 e #211(SOS-II). In red dots represent the Weddell Sea Shelf Water (WSSW).

Figure 6. Surface distributions of temperature (°C), salinity and upper mixed layer depth (UML) (meters) for (A, B, C) SOS-I Cruise, respectively, and for (D, E, F) SOS-II Cruise, respectively.

Figure 7. Surface distributions of *in situ* stimulated fluorescence (Relative Unit-RU), chlorophyll-a concentration ($mg \cdot m^{-3}$) and beam attenuation coefficient (660 nm) (m^{-1}) for (A, B, C) SOS-I Cruise, respectively, and for (D, E, F) SOS-II Cruise, respectively.

Figure 8. Relationship between Chlorophyll-a concentrations and salinity for SOS-I Cruise (black) and for SOS-II Cruise (gray). For the linear regression analyses presented here, only data from the mixed layer were used.

Figure 9. (A) Chla concentration vs fluorescence for SOS-I and SOS-II. Beam attenuation vs. derived Chla from fluorescence for (B) SOS-I and for (C) SOS-II. Black and gray dots and lines indicate linear fitting regressions for stations near the phytoplankton bloom (black dots), and stations far from the phytoplankton bloom (gray dots), #109, #110, #115, #118, #119 and #120 in SOS-I and for stations #209, #210, #211 and #212 in SOS-II, respectively. See text for statistical results.

Figure 1

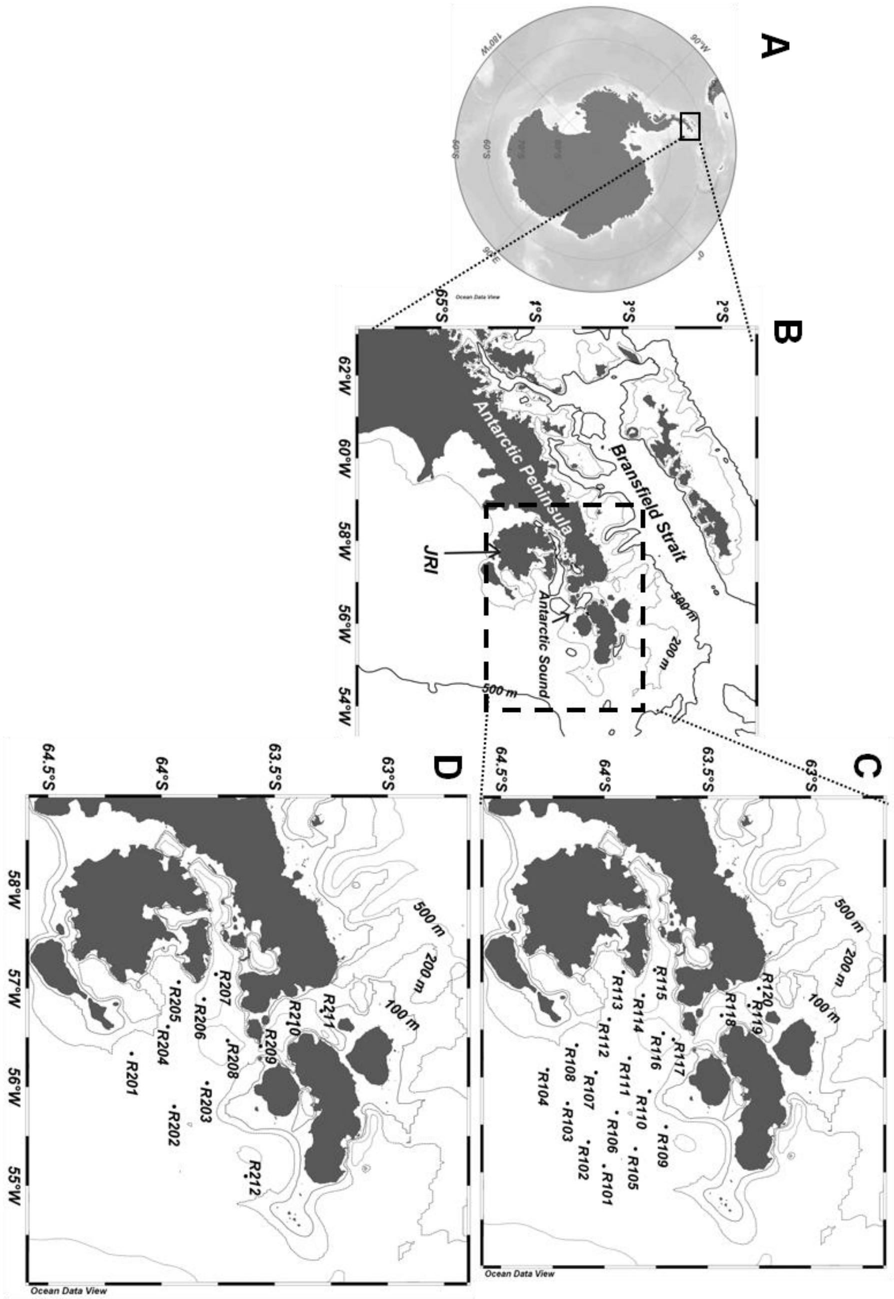
A
B
C
D
Antarctic Peninsula
Bransfield Strait
JRI
Antarctic Sound
500 m
200 m
100 m
62°W
60°W
58°W
56°W
54°W
57°W
55°W
64.5°S
64°S
63.5°S
63°S
R101
R102
R103
R104
R105
R106
R107
R108
R109
R110
R111
R112
R113
R114
R115
R116
R117
R118
R119
R120
R201
R202
R203
R204
R205
R206
R207
R208
R209
R210
R211
R212
Ocean Data View

Figure 2

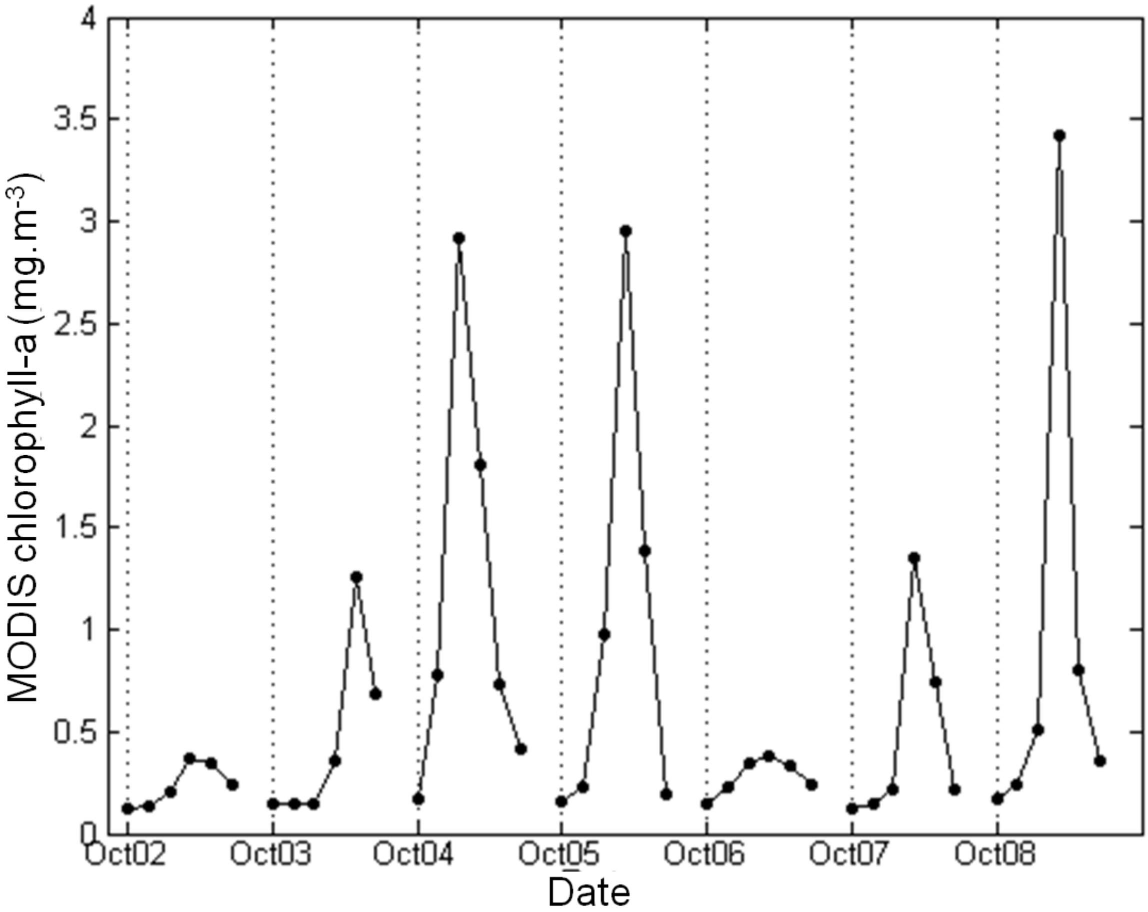
MODIS chlorophyll-a (mg.m-3)
0
0.5
1
1.5
2
2.5
3
3.5
4
Oct02
Oct03
Oct04
Oct05
Oct06
Oct07
Oct08
Date

Figure 3

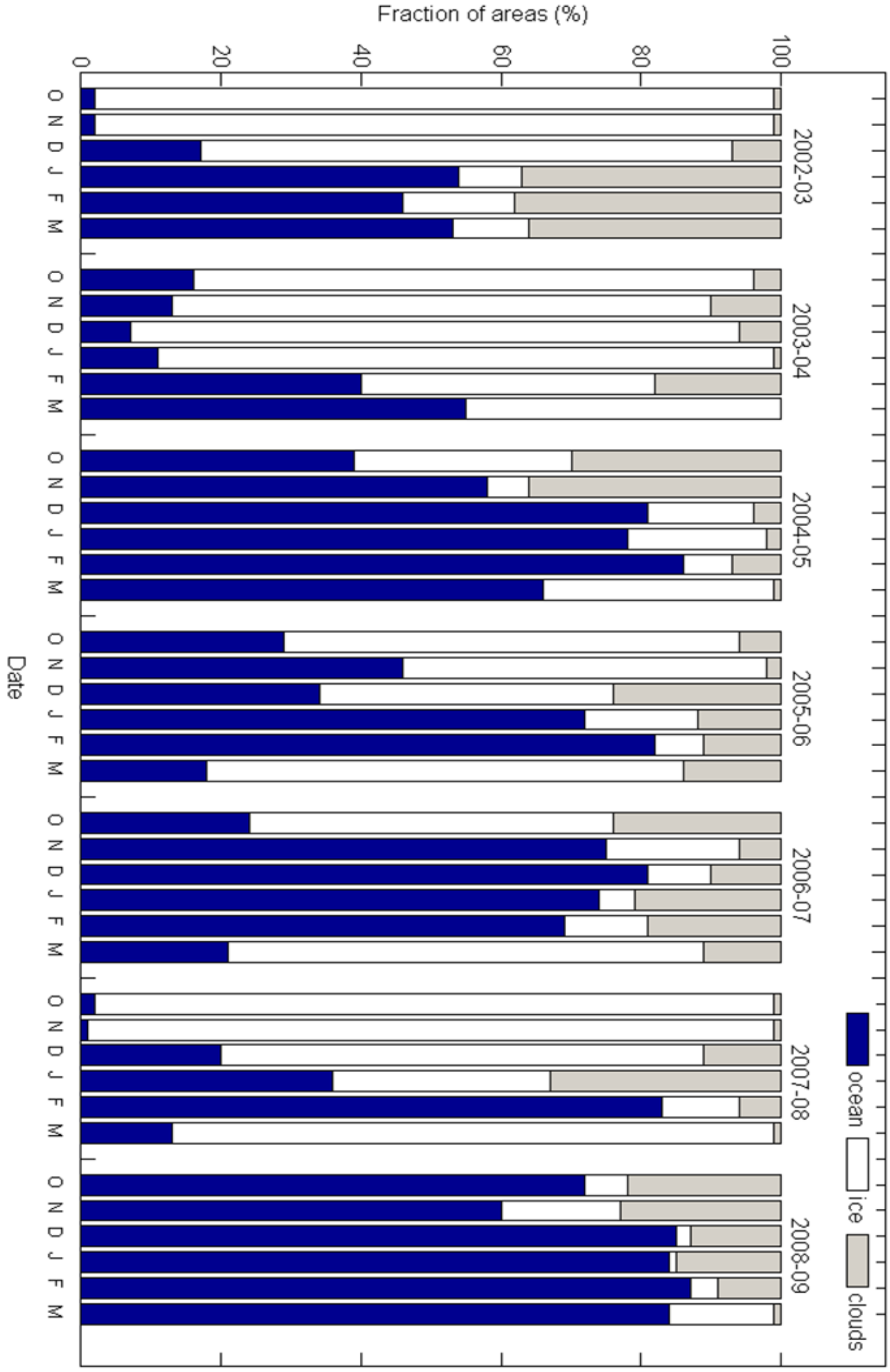
Fraction of areas (%)
0
20
40
60
80
100
Date
O N D J F M
2002-03
2003-04
2004-05
2005-06
2006-07
2007-08
2008-09
ocean
ice
clouds

Figure 4

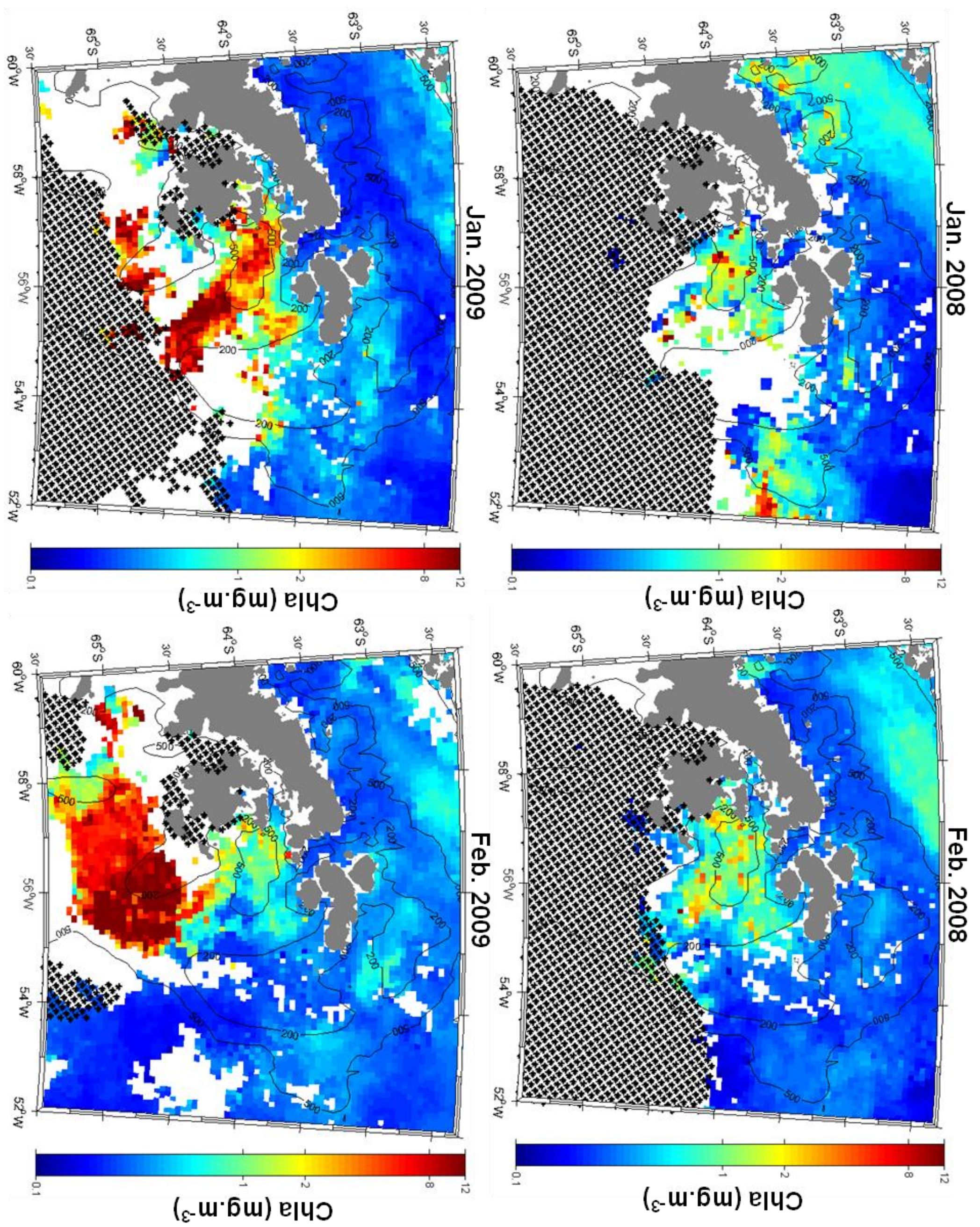

Figure 5

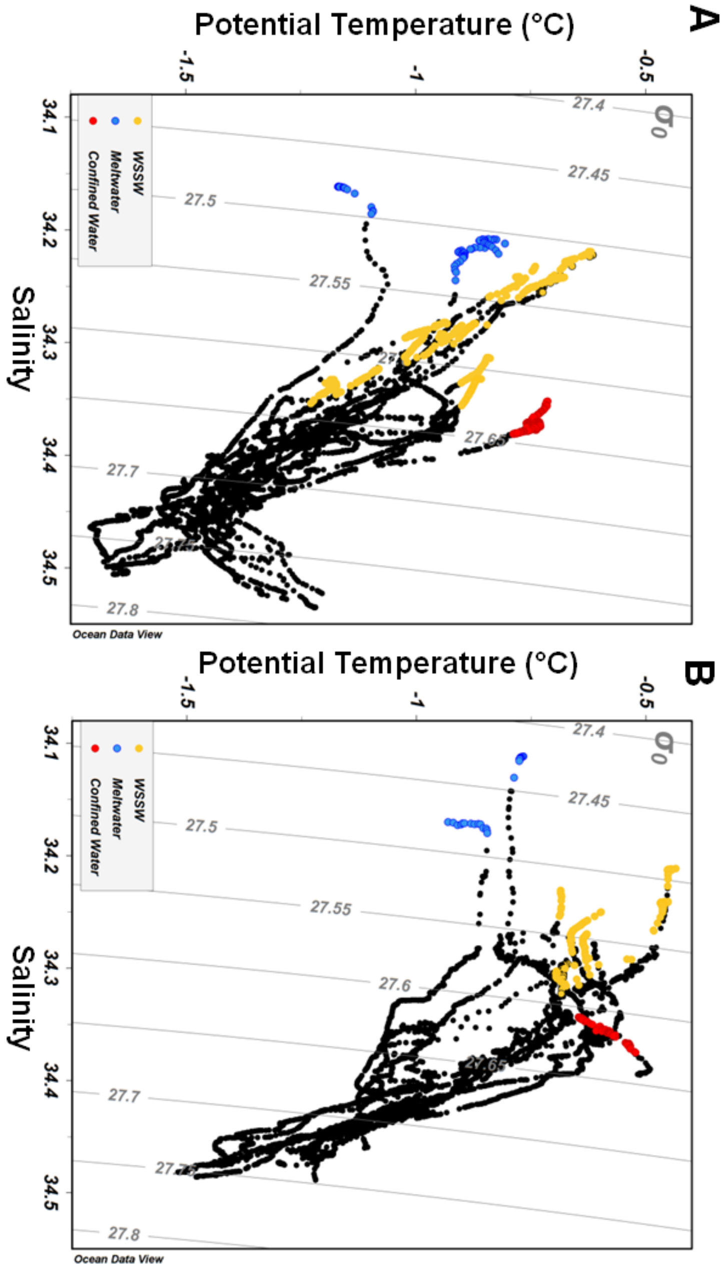
A
Potential Temperature (°C)
Salinity
WSSW
Meltwater
Confined Water
Ocean Data View
B
Potential Temperature (°C)
Salinity
WSSW
Meltwater
Confined Water
Ocean Data View

Figure 6

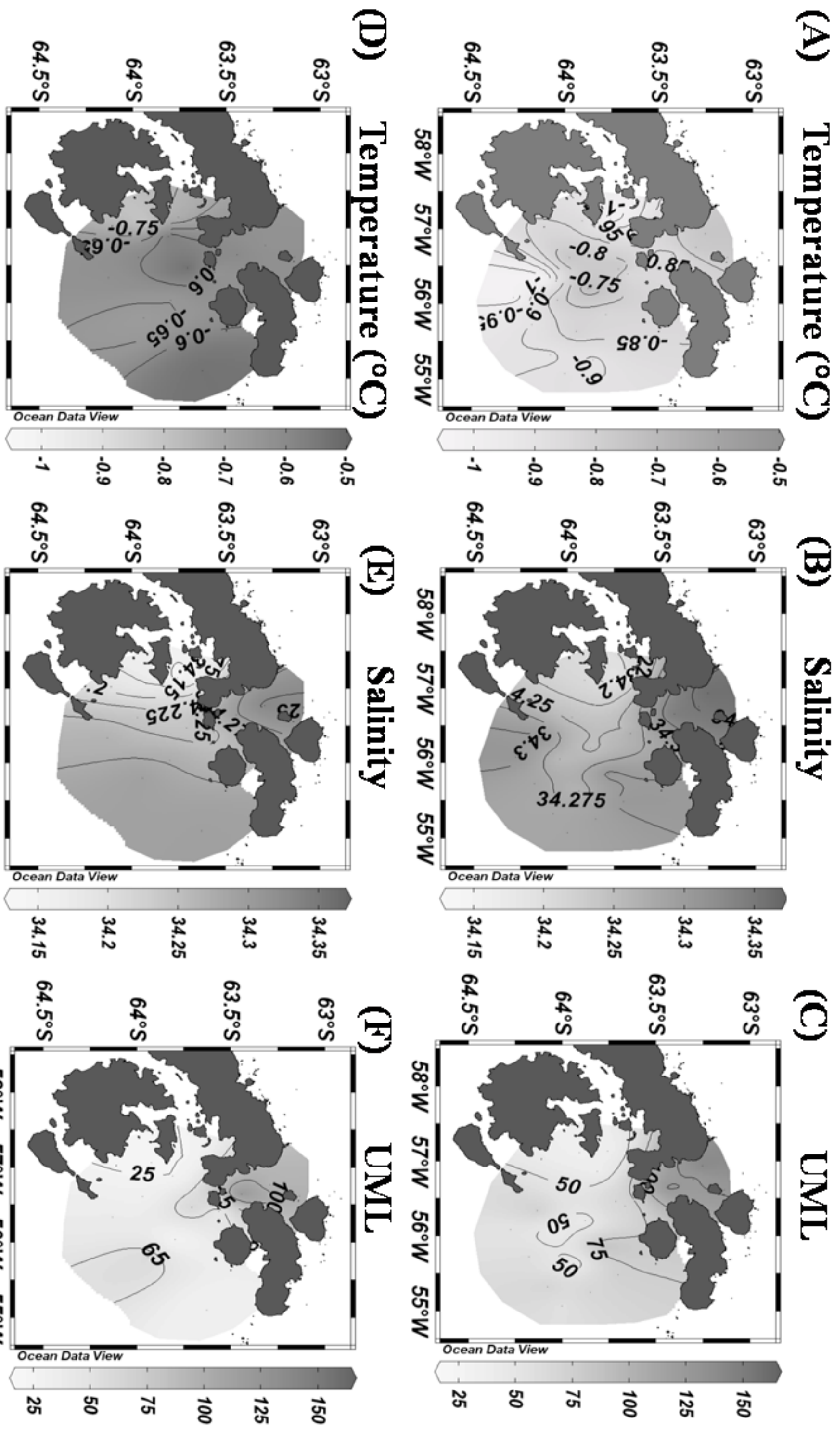
(A) Temperature (°C)
(B) Salinity
(C) UML
(D) Temperature (°C)
(E) Salinity
(F) UML
Ocean Data View

Figure 7

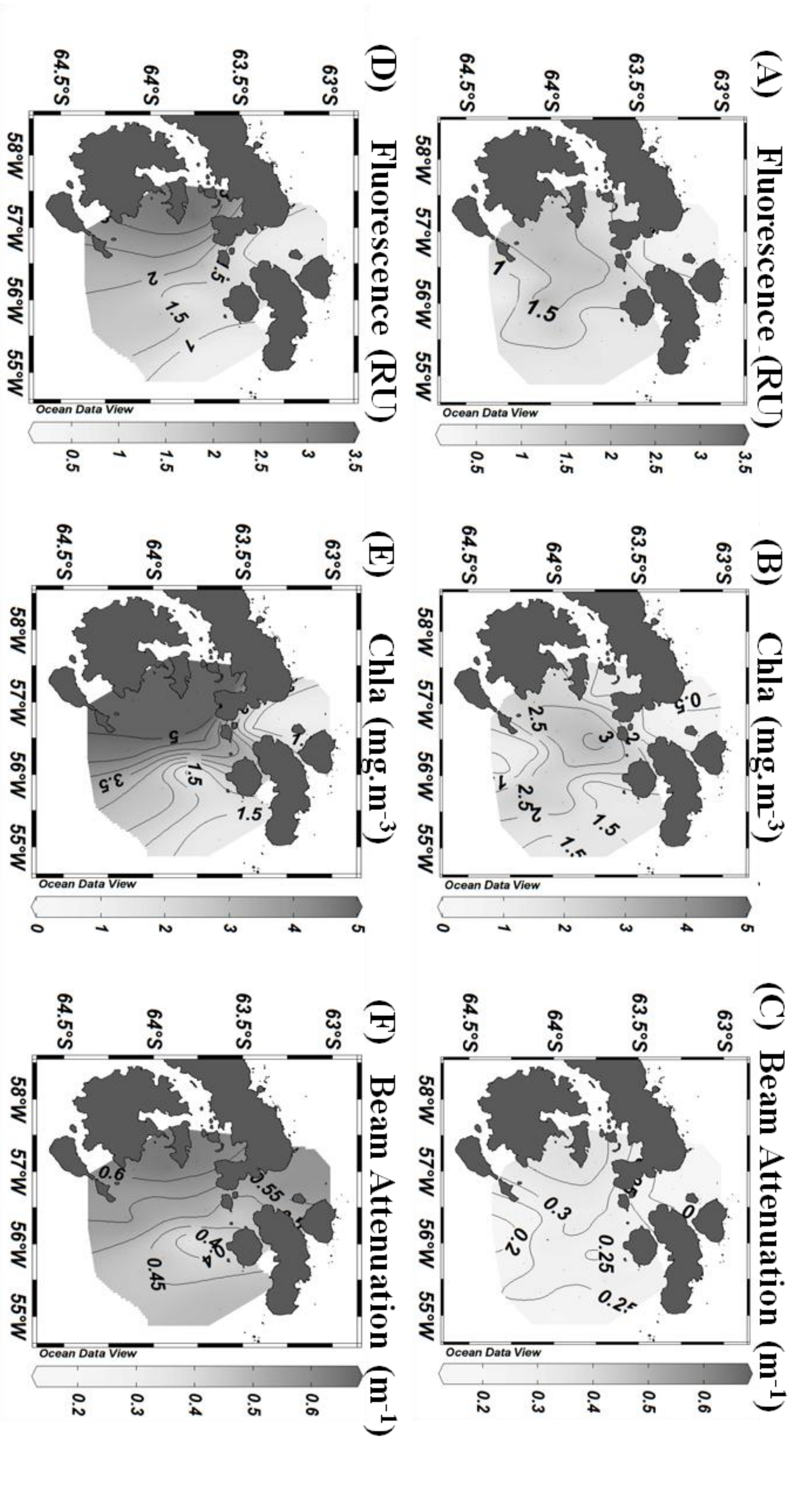
(A) Fluorescence (RU)
(B) Chla (mg.m-3)
(C) Beam Attenuation (m-1)
(D) Fluorescence (RU)
(E) Chla (mg.m-3)
(F) Beam Attenuation (m-1)
Ocean Data View

Figure 8

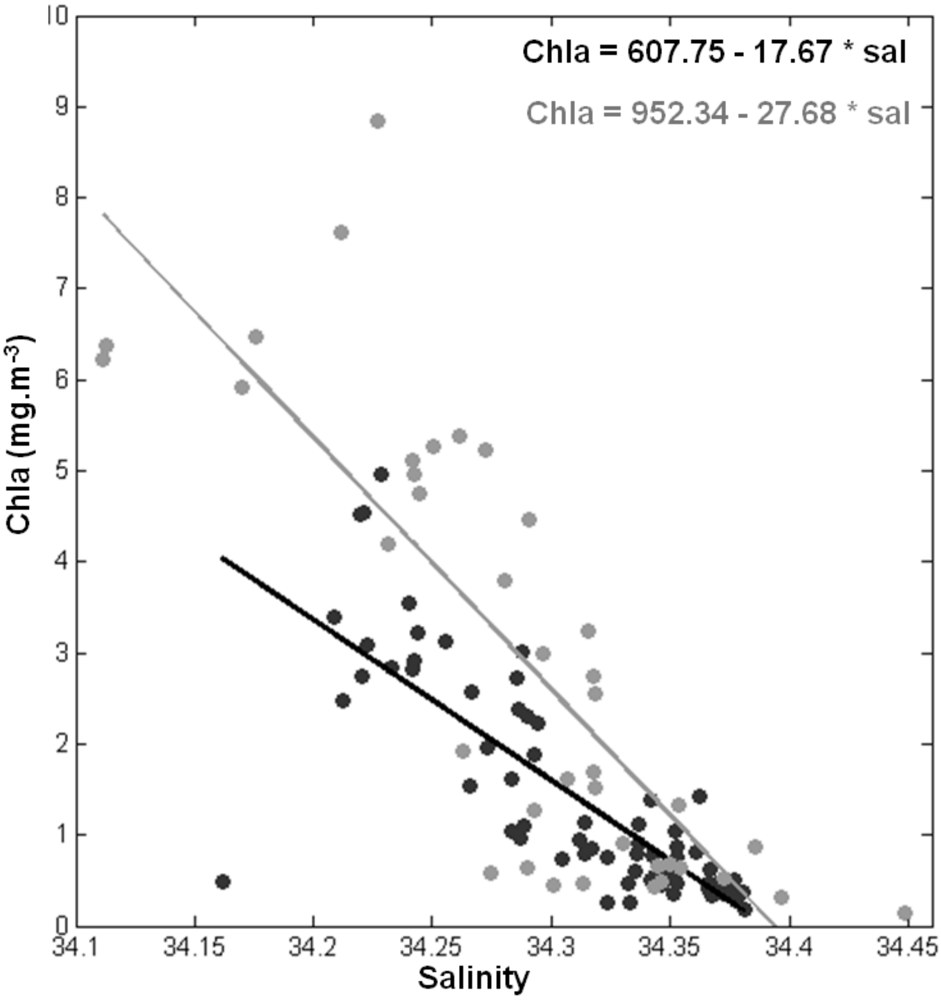
Chla = 607.75 - 17.67 * sal
Chla = 952.34 - 27.68 * sal
Chla (mg.m-3)
Salinity
10
9
8
7
6
5
4
3
2
1
0
34.1
34.15
34.2
34.25
34.3
34.35
34.4
34.45

Figure 9

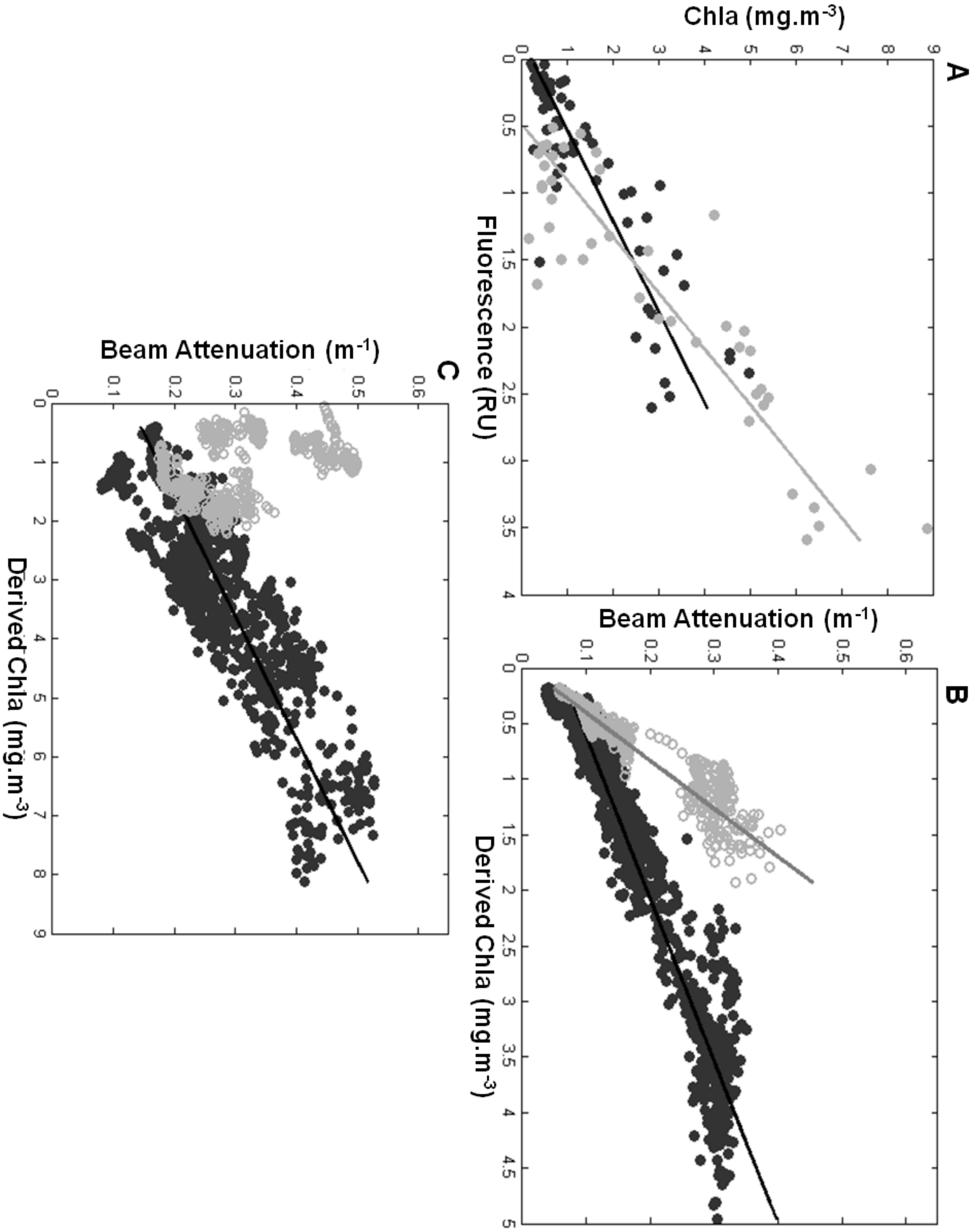
A
Chla (mg.m^{-3})
Fluorescence (RU)
B
Beam Attenuation (m^{-1})
Derived Chla (mg.m^{-3})
C
Beam Attenuation (m^{-1})
Derived Chla (mg.m^{-3})

Apêndice 2. **MANUSCRITO: formatado para o periódico Antarctic Science.**

Observational changes in the marine environment in the vicinity of a drifting iceberg in the northwestern Weddell Sea

Amália Detoni[a*]

Carlos A. E. Garcia[a]

Virginia M. T. Garcia[b]

Mauricio M. Mata[a]

Michael P. Schodlok[c]

Ricardo C. G. Pollery[d]

[a]Laboratory of Climate and Oceans Studies

[b]Laboratory of Phytoplankton and Marine Microorganisms

Institute of Oceanography

[c]JIFRESSE/University of California Los Angeles

[d]*Laboratory of Biogeochemistry / UFRJ*

Federal University of Rio Grande, Av. Italia, km 8, Rio Grande, RS, 96201-900, Brazil,

e-mail: amaliadetoni@gmail.com, dfsgar@furg.br, docvmtg@furg.br, mauricio.mata@furg.br, mschodlok@ucla.edu, pollery@hotmail.com

[*]Corresponding author: Tel. +55 53 32336617, Fax +55 53 32336887, e-mail: amaliadetoni@gmail.com

Abstract

Southern Ocean icebergs are formed in coastal environments after calving of shelves and drifting icebergs deliver particles that were incorporated in the Antarctic ice sheet from which the iceberg originated over. Water immediately surrounding icebergs may affect phytoplankton growth conditions by acting as a source of nutrients and controlling surface layer stratification. Drifting icebergs may negatively impact productivity by creating a physical barrier to normal sea ice advection patterns. In February 2009, an iceberg was tagged with a GPS buoy on the north-western Weddell Sea continental shelf, and 6 hydrographic stations were sampled to conduct physical, chemical, and biological measurements. Three stations were sampled south, and 3, sampled north of the iceberg, presumably before and after iceberg passage, respectively. The drifting iceberg destabilized the thermohaline structure north of its passage in shallow regions, causing turbulent mixing processes in the surface layer to a 250m depth. The water column was stable south of the iceberg, although our data indicate there was re-suspension of microalgae cells with active photosynthetic pigments from the sea-floor sediment. Micronutrients were also re-suspended from the bottom, without reaching the photic layer. The passage of the iceberg may drastically affect the water column in shallow environments by disturbing the bottom, revolving sediments, and re-suspending macronutrients and phytoplankton after they have been deposited.

Keywords: phytoplankton, thermohaline structure, melt-water, Weddell Sea, micronutrients.

1. Introduction

Icebergs are acknowledged to be potential sources of trace metals in surface waters where they drift and melt, releasing a load of particulates that were incorporated within the ice sheet from which the iceberg originated (Löscher *et al*., 1997, Smith *et al*., 2007). Waters immediately surrounding these icebergs are proposed to affect phytoplankton growth conditions in the Southern Ocean (Arrigo & Dijken, 2004, Smith *et al*., 2007, Schwarz & Schodlok, 2009).

An iceberg formed in a coastal environment in the Southern Ocean may take a long time to drift out of the region of origin (Schodlok *et al*., 2006, Jansen *et al*., 2007), and while drifting it will deliver fresh water, dust, and micronutrients, mainly iron, from terrigenous material of its origin (Arrigo & Dijken, 2004). Arrigo & Dijaken (2004) suggested that a consequence of these long residence times is that many icebergs were presumably located in highly productive coastal waters during the peak growth seasons of spring and summer. Their presence can alter the normal advection patterns of annual sea ice and hence the fraction of open water available for phytoplankton growth as well as the local ocean circulation (Grosfeld *et al*., 1998). However, because iceberg melt rates in the southern and western Weddell Sea are rather small (Jansen *et al*., 2007, Schodlok *et al*., 2006), it is unknown whether the dominant influence is the nutrient-rich melt-water or the nutrient-rich water up-welled in the vicinity of the iceberg.

Free drifting icebergs can act as sources of nutrients (including iron) and can control the stratification of the surface layer in surrounding waters. Low-salinity melt-water produces low-density surface waters that reduce vertical mixing and creates a shallow upper mixed layer, providing excellent conditions for high primary productivity

(Garibotti *et al*., 2003; Boyd, 2002; Marrari *et al*., 2008). Hence, drifting icebergs increase local primary production and thereby carbon sequestration by biological activity in the Southern Ocean (Smith *et al*., 2007; Schwarz & Schodlok, 2009).

In addition, icebergs may act as physical barriers to the normal advection patterns of sea ice in their vicinity (Arrigo & Dijken, 2004) and may negatively impact the environment for phytoplankton growth. If icebergs pass through a well-stratified water column with a high phytoplankton biomass in the upper layer, they could produce the contrary effect by destroying the stable surface layer and thus force phytoplankton cells to adapt to lower light levels (Schwarz & Schodlok, 2009).

Schwarz & Schodlok (2009) revealed that the keel of an adrift iceberg causes turbulent mixing, potentially enabling the transfer of thermal energy, nutrients, phytoplankton cells, and water of different salinity across the pycnocline (the base of the mixed layer). The degree of turbulence is determined by the topography of the keel of the iceberg and by the relative velocity between the iceberg and the surrounding water (Jansen *et al*., 2007). Thus, an initially high concentration of phytoplankton cells near the ocean surface could be mixed through the water column by the passing iceberg, decreasing the surface pigment concentration.

Smith *et al.* (2007) recently compared these icebergs to ‘Lagrangian estuaries’ because they supply nutrients and upper layer stability to the surrounding waters. They proposed that icebergs and their associated communities could serve as areas of increased production and sequestration of organic carbon to the deep sea.

The frequency of icebergs in the north-western Weddell Sea has increased as a consequence of the disintegration of the Larsen ice shelves at the Antarctic Peninsula (Smith *et al*., 2007). Although the majority of icebergs are of small to medium scale, some icebergs have larger dimensions and reach areas greater than 200 km^2. Smith *et al.* (2007) suggest that the proliferation of icebergs associated with global warming should markedly increase their influence on the Southern Ocean ecosystem and thereby on carbon sequestration.

Numerical studies of iceberg drift have addressed the impact of time- and space-variable ocean drag, wind drag, the Coriolis effect, and other drift forces as a steering influence of the sea ice movement on the iceberg (Gladstone *et al*., 2001, Lichey & Hellmer, 2001). Close to the Antarctic Peninsula, the drift is more uniformly northward with little meandering (Schodlok *et al*., 2006). Gladstone *et al.* (2001) demonstrated that trajectories simulated by a numerical model show a high degree of entrainment of icebergs within the coastal current around almost the entire Antarctic coastline. Additionally, near the tip of the Antarctic Peninsula (~55°W) is a region where the movement of icebergs away from the coast is most frequent. The main cause of northward movement in those regions is topographic steering affecting ocean currents. Icebergs near the coast will be subjected to a mixture of the east wind drift and katabatic winds (King & Turner, 1997).

Various numerical studies tracked and/or monitored icebergs by satellite images with various sensors to describe the trajectories of icebergs and/or the influence of melt-water from an iceberg on phytoplankton growth into the water column (Arrigo & Dijken, 2004, Schodlok *et al*., 2006, Jansen *et al*., 2007, Smith *et al*., 2007, Schwarz & Schodlok, 2009); however, these studies showed only the first centimeters of the water column and therefore might have missed part of the picture.

In this article, we report the environmental conditions in the surrounding waters of an iceberg near the Antarctic Peninsula. After the iceberg position was accurately recorded by a GPS system, we carried out a survey in the waters south and north of the iceberg. The cruise was conducted on board the Brazilian R.V. Ary Rongel where physical, optical, and biogeochemical properties were measured to characterize the environmental conditions to the south and to the north of the iceberg. From the surrounding distribution of icebergs and the drift of the present iceberg, we presumed that the locations to the south, but not to the north, were subject to iceberg influence.

The chosen iceberg was drifting within the study area north-east of the Antarctic Peninsula in coastal waters close to the tip of the Antarctic Peninsula (Fig.1). This region is usually covered by sea ice and presents a marginal ice zone of high phytoplankton biomass and productivity in satellite images (Park *et al*., 1999).

The Antarctic Peninsula offers an important barrier to westerly winds, therefore the south coastal winds in late spring and summer, associated with northward flow of the Weddell Sea Shelf Water (WSSW) promote drift of icebergs in the north-west in the study area. The potential release of iron from glaciers and melting icebergs adds to the stability of water column and favours seasonal phytoplankton bloom in the region, which is usually observed on ocean satellite daily image (Fig. 2).

Our main goal was to address the impact of a drifting iceberg by examining the physical, optical, chemical, and biological characteristics of the surrounding waters.

The study was conducted during austral summer 2009 (19–20 February) as part of the project ‘Southern Ocean Studies for Understanding Global Climate Issues (SOS-CLIMATE)’, a Brazilian contribution to the International Polar Year.

2. Material and Methods

In February 2009, we placed a buoy (manufactured by Optimare Sensorsysteme GmbH, Bremerhaven, Germany) on top of an iceberg that transmitted its GPS positions via the ARGOS satellite system over an 8-hour ARGOS transmission window. The tabular iceberg, which was chosen by visual inspection, had dimensions of approximately 1.78 km length and 1.39 km width, and 45 m freeboard was tagged in sea ice free waters at about 64°14.45'S, 55°27.10'W in the north-western Weddell Sea near James Ross Island (Fig. 1).

This region of the Weddell Sea is characterized by an abundance of icebergs that primarily originated from calving of the ice-shelf edge and drift with the Weddell Gyre northward (Schodlok *et al*., 2006). However, in February 2009, few icebergs were located in the vicinity of the tagged iceberg. This allowed us to distinguish an area that was most likely influenced (south of the iceberg) and an area most likely not influenced (north of the iceberg) by the iceberg in terms of melt-water and/or turbulence due to drift, to obtain hydrographic samples. Tide model results for the Scotia Sea indicate that tidal currents are of the expected order of magnitude in shallow areas (Robertson *et al*., 1998). Bathymetric features near James Ross Island are shallow, and therefore, we assumed that the tidal conditions were comparable. Jansen *et al.* (2007) stated that a grounded iceberg is subject to tidal currents, the cold water plume erodes with the tidal cycle, and the temperature leads to effective melting.

The tagged iceberg position is shown in Figure 2(A) in the MODIS-Aqua image that corresponds to the day after the berg was tagged, and Figure 2(B) shows the positions of the hydrographic stations in relation to the tabular iceberg in the radar image of the same day (Advanced Synthetic Aperture Radar – ASAR from ENVISAT). The MODIS image shows that many icebergs of various sizes were present in the north-western Weddell Sea but that only 2 smaller icebergs were in the immediate vicinity.

We occupied 6 oceanographic stations (#I201 – #I206) in the peripheral waters of the selected free-drifting iceberg. The tagged iceberg was drifting in the north-east direction while the oceanographic studies were being performed (Fig. 3B). The region south of the study area presented high chlorophyll-a concentrations (Fig. 3A) (MODIS-Aqua 20 February 2009), but the tagged iceberg location was outside of the phytoplankton bloom. The red marker in the ocean colour image represents the tagged iceberg location within waters with low chlorophyll-a concentration.

Three conductivity, temperature, and depth (CTD) hydrographic stations, with water sampling for chemical and biological analyses, were located in the north of the iceberg, and the other 3 were located to the south of the free-drifting iceberg. Analysis of chlorophyll-a in the water column was performed in 2 stations to the south (#I201 and #I203), and 2 stations to the north (#I204 and #I206) of the iceberg.

2.1. Oceanographic Data

The vertical profiles of temperature, salinity, fluorescence, and beam-attenuation *c* (660 nm) were taken with a Sea-Bird CTD/Carrousel 911+ system in the 6 stations.

The track of the iceberg from 19 February to 1 June is shown in Figure 4, after which the record stopped because of a malfunctioning buoy or capsizing of the iceberg and loss of the instrument.

The upper mixed layer depth (UML) was calculated according to Hewes *et al.* (2008); however, an adjustment was necessary because the maximum differential σ-t along the water column, corresponding with the pycnocline in our data set was found at 0.08 kg·m^{-3}, while in Hewes *et al.* (2008) was by 0.05 kg·m^{-3}.

The density profile in the study region is more associated with the salinity than the temperature profile. The difference of density between the first station and the last station were significant within a depth of 250m (~0.08 km·m^{-3}). Thus, to characterize the different density profiles of the farthest stations from iceberg, we considered data from the surface to a depth of 250m.

2.2. Measurement of chlorophyll-a and nutrients

Seawater samples of 0.5–1 L were filtered onto Whatman 25mm GF/F filters and immediately stored in liquid nitrogen. Photosynthetic pigments were extracted with 2 mL of 95% cold-buffered methanol (2% ammonium acetate) for 30 min at –20°C in the dark. The samples were sonicated (Bransonic, model 1210) and centrifuged. Extracts were filtered (Fluoropore PTFE filter membranes, 0.2μm pore size) and immediately analyzed in the HPLC system. The HPLC method, based on a monomeric C8 column and a pyridine-containing mobile phase, followed the method of Zapata *et al.* (2000) and the adaptation by Mendes *et al*. (2007).

Chlorophyll-a concentration was calculated from the signal in the photodiode array detector and the HPLC system was calibrated with a Sigma commercial standard. The pigment was identified from absorbance spectra and retention times and concentrations were calculated from the signals in the photodiode array detector or fluorescence detector (Ex. 430nm; Em. 670nm).

Concentrations of essential micronutrients (silicate, phosphate, and nitrate) were measured at 8 established depths (5, 25, 50, 100, 150, 200, 250, and 327m). The analyses were performed in the laboratory of the Brazilian R.V. Ary Rongel using the colorimetric method. Determination of nutrient concentration was based on the protocol recommended by Aminot & Chaussepied (1983).

3. Results and Discussion

3.1 Environmental Conditions and Iceberg Movement

The position of the iceberg in reference to the CTD–specific stations enabled us to calculate the displacement of the iceberg during the study period, and its speed was estimated at approximately 6.5 km/d.

In physical terms, the force of the wind causes the iceberg to move at a different speed than the surrounding ocean currents (Gladstone *et al*., 2001). Wind data collected on board the ship during the cruise showed that the wind speed during the time of the hydrographic sampling increased from 7.20m·s^{-1} to 10.29m·s^{-1} from the southwest, in the first 2 stations (#I201 and #I202) before slightly changing its direction approximately 20° to the south-southwest. Wind speed decreased from 8.23 m·s^{-1} to 6.17 m·s^{-1} in the last stations (#I205 and #I206), but continued from the southwest direction. The direction of iceberg motion during the sampling remained at north-northwest.

Baines (2006) reported that components of the diurnal tide (K_1 – Luni-solar diurnal and O_1 – Principal lunar diurnal) have amplitudes of approximately 0.4 m in the Weddell and Ross Seas, and there is evidence of diurnal tidally-forced continental shelf waves near the shelf break in the Southern Weddell Sea, apparently generated by diurnal tidal currents interacting with local topographic features. We have no data regarding tidal cycle or eddies observed in the area, but these features may explain the iceberg behaviour (more information see Collares *et al*., 2011 in preparation). However, Gladstone *et al.* (2001) state that the meso-scale wind force induces small meanders in iceberg trajectories, causing a greater proportion of icebergs to leave the coastal current.

The iceberg moved primarily east in the beginning, and drifted north-west during the 11 h after it was tagged. The iceberg motion during the period from 19 Feb. to 1 Jun. is shown in Figure 4. The motion suggests that the iceberg was probably following the complex surface currents and showing behaviour that imparted irregular spiralling rotations before it finally drifted in the north-western direction.

The speed of the iceberg was 0.26 $m \cdot s^{-1}$ between the #I201 and #I202 measurements, which was the faster displacement of the iceberg in the surrounding stations's regions compared to speeds of iceberg trajectory during the experiment.

3.2 Physical Properties of the Water Column and T/S Diagram

Greater stratification and stability of the water column were observed in stations south of the iceberg. Lower salinity, density, and temperature were observed in the surface waters (the first 20m depth) of these stations (Fig. 5). It is possible that the melt-water of the iceberg re-stabilized the water column by creating a wake of freshwater in the surface (temperature, approximately -0.84°C; salinity, < 34.2).

The T/S diagram comprising stations that were presumably affected by the iceberg passage (south) is presented in Figure 6A, including the furthest north station (#I206), which presented similar thermohaline structure. Figure 6B shows T/S diagram corresponding to the remaining stations north of the iceberg. The nearest stations, #I204 and #I205 showed peculiar temperature and salinity profiles (Fig. 6B). We also observed instability of the thermohaline structure in the upper water column in stations #I205 and #I204 from the surface to 100 m and to 265m, respectively, with the presence of low salinity surface water (approximately 34.2).

In 3 stations south of the iceberg (#I201 to #I203), and in station #I206, we observed the presence of Weddell Sea Shelf Water (WSSW) (Fig. 6A) with a characteristic temperature of -1.3°C – -0.7°C and salinity > 34.2. This water follows a surface current which flows partly north-west toward the Antarctic Peninsula and the other part flows north toward the Antarctic Convergence (Sañudo-Wilhelmy *et al*., 2002). The WSSW is generally present from the surface to a depth of approximately 300 m, into the water column of the continental shelf of the Weddell Sea. However, the WSSW appears from the 20m depth in the southern stations, presumably because the iceberg melt-water is present in the first 20m depth in the water column.

A comparison of the density profiles in the first 250m depth of the stations furthest from the tagged iceberg (#I201 to southern and #I206 to northern) is shown in Figure 7. The first station (#I201) has lower surface density, indicating higher stratification in the water column than the last station (#I206), which has higher surface density and presumably was not influenced by iceberg melt-water. However, the T/S of #I206 and #I201 showed a similar thermohaline structure down to the first 20m depth.

In stations #I204 and #I205, which were closer to the iceberg and exhibited instability of the thermohaline structure, we observed a slight decrease in salinity and density in the upper water column (the first 20m), compared to the south stations and Station #I206 (Fig. 6B). Presumably, there was a mixture of the WSSW with the freshwater input from the melting iceberg, leading to strong turbulent mixing from iceberg drag. Schwarz & Schodlok (2009) stated that near the coast, the submersed part of the iceberg may be sufficient for the iceberg to be grounded, potentially disturbing circulation patterns, sea ice formation, and consequently the entire ecosystem. Once an iceberg is adrift, the keel causes turbulent mixing, potentially enabling the transfer of salinity, thermal energy, nutrients, and phytoplankton cells across, the base of the mixed layer (the pycnocline) (Schwarz & Schodlok 2009).

Thus, an iceberg may influence the thermohaline structure not only by melting water input, but also by the topography of the keel of an iceberg and by the relative velocities of the iceberg and the surrounding water (Pisarevskaya & Popov, 1991, Schwarz & Schodlok, 2009). The melting effects could be the region of trapped fluid in front of the moving iceberg and the turbulence effects (Pisarevskaya & Popov, 1991). Figure 7 illustrates the effect of with a deep keel passing through deeply-mixed waters, altering the density structure of the upper water column, forming a stable lens of less dense water.

Our results suggest that the melt-water from the iceberg created stratification of water columns with low densities (a decrease of $0.08 kg \cdot m^{-3}$) and low temperatures (a decrease of 0.06°C) in surface water due to the input of melt-water. This led to the re-stabilisation of the thermohaline structure with shallowing of the upper mixed layer, while stations #I204 and #I205 were disturbed with instability of thermohaline structure and turbulent mixing of the surface layer to a depth of approximately 250m.

3.3. Biological Properties of the Water Column

The hydrographic stations located north of the track of the iceberg (#I204 to #I206), where we assume that the iceberg did not pass, showed profiles with moderated chlorophyll-a concentrations below 150 m (circa $0.5 mg \cdot m^{-3}$). For instance, #I204 had a $0.48 mg \cdot m^{-3}$ chlorophyll-a concentration at 200m depth, while surface values were 0.12 to $0.24 mg \cdot m^{-3}$. This was also observed by stimulated fluorescence profiles throughout the water column (Fig. 8), where the largest concentrations were found below a depth of

150 m (1mg·m^{-3}). However, the #I206 station presented the lowest chlorophyll-a concentration at the surface (0.2mg·m^{-3}), associated with deeper upper mixed layer (56 – 89m).

In contrast, the profile of stations #I201 to #I203, which were located south of the track of the iceberg, showed a major stimulated fluorescence gradient below 130 m depth (Fig.8), specially #I201. The phytoplankton biomass, inferred as chlorophyll-a concentration, was greater below a depth of 200 m (> 0.45mg·m^{-3}) than at surface. These stations showed a shallower upper mixed layer depth (43–53m), as well as the likely stratification of the water column. In the #I201 station, the biomass was 0.6mg·m^{-3} at a depth of 250m, and this curiously high value was consistent with stimulated fluorescence and beam attenuation values.

The high chlorophyll-a concentration down to a depth of 200 m may have resulted from the passage of the iceberg before it was tagged, creating favourable conditions for the surface growth phytoplankton bloom, and the biomass that was not grazed by zooplankton was deposited at the bottom. The study area was approximately 400m deep and because of the size of the freeboard of the iceberg; it is possible that the tagged iceberg drifted close to the sea floor. When the tagged iceberg drifted, it may have re-suspended the cells above the bottom within the water column, which resulted in active photosynthetic pigments.

Schwarz & Schodlok (2009) demonstrated that iceberg transit could cause high stratification, and that iceberg-induced mixing presumably mixes the surface population down to greater depths, causing an apparent loss of surface biomass. The formation of a deep chlorophyll maximum at depths greater than 50m is generally attributed to either (1) a nutrient limitation, where the chlorophyll-a maximum develops at the base of the nutricline for the limiting element, or (2) the setting of phytoplankton to deeper water, which may happen after the occurrence of rich phytoplankton bloom in surface waters (Holm-Hansen *et al*., 2005).

Phytoplankton species in polar regions that have adapted to prolonged darkness can live in greater depths. At these conditions of low light intensity, the phytoplankton cells are normally smaller in size and have more chlorophyll pigments per cell, thereby giving the appearance of a high biomass when measured by stimulated fluorescence in the field. The survival of these microorganisms consists of structural, physiological, and biochemical changes at the cellular level, which involve the photosynthetic apparatus (Baldisserotto, 2005). Therefore, in our study, the iceberg may have caused suspension of cells if they were in the sediment of shallow areas, and these cells showed active photosynthetic pigments.

3.4 Nutrients

Vertical profiles of the main nutrients (nitrate, phosphate and silicate) are shown in Figure 9. The nutrient distribution exhibited a similar pattern to chlorophyll-a concentration. The nitrate and silicate concentrations were higher at depth than at the surface, especially in #I201. Station #I201 showed nitrate values of 25µM (at surface) and 33.8µM (at depth), and silicate values of 59.8 µM (at surface) to 67µM (at depth), under influence of iceberg drift (Fig. 9). The northern stations showed lower nitrate and silicate concentrations (Fig. 9) than the southern stations, but these nutrients were all higher at depth and lower at surface, which is a normal condition in marine ecosystems because of decomposition of sedimented organic matter. Much of the organic carbon deposited at high latitudes occurs during the spring and summer bloom periods, and the organic material in marine sediment is largely composed of high molecular weight compounds not readily available for bacterial uptake (Mincks *et al*., 2005). These authors reported that the microbial biomass varied only slightly with the season, and most of the variability was confined to the top 3–4cm of the sediment and the phytodetritus layer. Thus, in shallow areas, the deposition of organic particulate material, and the revolving of bottom sediments might enrich waters near the bottom.

The significant increase of nitrate and silicate concentrations that appeared at depth in the southern stations suggests that the passage of the iceberg may have caused revolving of the bottom sediments, and made available the organic matter for deeper waters, that was previously deposited. This was not observed for phosphate, whose higher values were found in the north stations (Fig. 9), and at depths bellow 200m. Based on data from phytoplankton pigments and nutrients such as nitrate and silicate, it can be inferred that free-drifting icebergs may re-suspend the microalgae cells from sediment and probably provide organic matter and inorganic nutrients for benthic organisms.

4. Conclusions

Our data indicate that there is a wake with melting water behind the iceberg passage that provides re-composition of water column stability and returns the stratification of the thermohaline structure, thus forming a shallow mixed layer. On the other hand, it promoted turbulence and mixing in the upper water column in its immediate path. In shallow waters, such as the study area, the keel of the iceberg can be sufficiently deep to drag the sea bottom while drifting, revolving the sediment and re-suspending nutrients and phytoplankton cells. In our study, there was indication that this process occurred, based on detection of phytoplankton pigments (chlorophyll-a) and nutrients (nitrate and silicate) near the bottom, at stations south of the iceberg. Therefore, we conclude that drifting icebergs can have important influences on the surrounding ecosystem, modifying physical water column structure and, in shallow waters, disturbing biota and chemistry of the near-bottom environment.

Acknowledgments

This research work is part of GOAL (Group of High Latitude Oceanography) activities and was support by the funding resources of CNPq (Brazilian National Council on Research and Development) and MMA (Ministry of Environment) to the Brazilian Antarctic Program (PROANTAR). The authors would like to thank the crew of the Brazilian Navy research ship "*Ary Rongel*" for their assistance and for contributing to the success of the cruise. We are very grateful to Rafael Mendes for HPLC analysis. This research is part of a master dissertation, with fellowship to AMSD from CAPES (Brazilian Coordination Agency for Improvement of High Level Personnel).

References

Aminot, A. & Chaussepied, M., 1983. Manuel des analyses chimiques en milieu marin. Brest, **CNEXO**, 379p.

Arrigo, K. R. & van Dijken, G. L., 2004. Annual changes in sea-ice, chlorophyll *a*, and primary production in the Ross Sea, Antarctica. Deep-Sea Research Part II. 51, 117-138.

Baines, P. G., 2006. Coastal and Regional Currents of Antarctica. Encyclopedia of the Antarctic. 2, 269-272.

Baldisserotto, C., Ferroni, L., Andreoli, C., Fasulo, M. P., Bonora, A. & Pancaldi, S., 2005. Dark-acclimation of the Chloroplast in *Koliella Antarctica* Exposed to a Simulated Austral Night Condition. Arctic, Antarctic, and Alpine Research. 37, 146-156.

Bidigare, R. R., Ondrusek, M. E., Kennicutt II, M. C., Iturriaga, R., Harvey, H. R., Hoham, R. W. & Macko, S. A., 1993. Evidence for a photo-protective function for secondary carotenoids of snow algae. Journal of Phycology. 29, 427-434.

Boyd, P. W. 2002. Environmental Factors Controlling Phytoplankton Processes in the Southern Ocean. Journal Phycology: An International Journal of Algal Research. 38, 844-861.

Garibotti, I. A., Vernet, M., Ferrario, M. E., Smith, R. C., Ross, R. M. & Quetin, L. B., 2003. Phytoplankton spatial distribution patterns along the western Antarctic Peninsula (Southern Ocean). Marine Ecology Progress Series. 261, 21-39.

Gladstone, R. M., Bigg, G. R. & Nicholls, K. W., 2001. Iceberg trajectory modeling and meltwater injector in the Southern Ocean. Journal of Geophysical Research. 106, 19903-19915.

Grosfeld, K., Hellmer, H. H., Jonas, M., Sandhäger, H., Schulte, M. & Vaughan, D. G., 1998. Marine ice beneath Filchner Ice Shelf Evidence from a multidisciplinary approach. Ocean, Ice and Atmosphere interactions at the Antarctic continental margin. Res. Ser., 75, edited by S. S. Jacobs, and R. F. Weiss, 319-339, AGU, Washington, D. C.

Hewes, C. D., Reiss, C. S., Kahru, M., Miltchell, B. G. & Holm-Hansen, O., 2008. Control of phytoplankton biomass by dilution and mixed layer depth in the western Weddell-Scotia Confluence. Marine Ecology Progress Series. 366, 15-29.

Jacobs, S. S. & Comiso, J. C., 1989. Sea ice and oceanic processes on the Ross Sea Continental Shelf . Journal of Geophysical Research. (C12), 195-211.

Jansen, D., Schodlok, M. & Rack, W., 2007. Basal melting of A-38B: A physical model constrained by satellite observations. Remote Sensing & Environment. 111, 195-203.

King, J. C. & Turner, J., 1997. Antarctic Meteorology and Climatology, Cambridge University. Press, New York.

Kirst, G. O. & Wiencke, C., 1995. Ecophysiology of polar algae. Journal of Phycology. 31, 181-199.

Lichey, C. & Hellmer, H. H., 2001. Modeling giant iceberg drift under the influence of sea ice in the Weddell Sea. Journal of Glaciology. 47, 452-460.

Löscher, B. M., De Baar, H. J. W., De Jong, J. T. M., Veth, C. & Dehairs, F., 1997. The distribution of Fe in the Antarctic Circumpolar Current. Deep-Sea Research II. 44, 143-187.

Marrari, M., Daly, K. L. & Hu, C., 2008. Spatial and temporal variability of SeaWiFS chlorophyll *a* distributions west of Antarctic Peninsula: Implications for krill production. Deep-Sea Research II. 55, 377-392.

Mendes, C. R., Cataxana, P. & Brotas, V., 2007. HPLC determination of phytoplankton and microphytobenthos pigments: comparing resolution and sensitivity of a C_{18} and a C_8 method. Limnology and Oceanography: Methods. 5, 362-370.

Mincks, S. L., Smith, C. R. & DeMaster, D. J., 2005. Persistence of labile organic matter and microbial biomass in Antarctic shelf sediments: evidence of a sediment 'food bank'. Marine Ecology Progress Series. 300, 3-19.

Park, M. G., Yang, S. R., Kang, S., Chung, K. H. & Shim, J. H., 1999. Phytoplankton biomass and primary production in the marginal ice zone of the northwestern Weddell Sea during austral summer. Polar Biology. 21, 251-261.

Pisarevskaya, L. G. & Popov, I. K., 1991. Free-drifting icebergs and thermohaline structure. Glaciers-Ocean-Atmosphere Interactions. 208, 447-454.

Robertson, R., Padman, L. & Egbert, G. D., 1998. Tides in the Weddell Sea. Ocean, Ice and Atmosphere interactions at the Antarctic continental margin. Antarctic Res. Ser., edited by S. S. Jacobs, and R. F. Weiss AGU, 341-369.

Sañudo-Wilhelmy, S. A., Olsen, K. A., Scelfo, J. M., Foster, T. D. & Flegal, A. R., 2002. Trace metal distributions off the Antarctic Peninsula in the Weddell Sea. Marine Chemistry. 77, 157-170.

Schodlok, M., Hellmer, H. H., Rohardt, G. & Fahrbach, E., 2006. Weddell Sea iceberg drift: Five years of observations. Journal of Geophysical Research. 111, C06018, doi:10.1029/2004JC002661.

Schwarz, J. N. & Schodlok, M. P., 2009. Impact of drifting icebergs on surface phytoplankton biomass in the Southern Ocean: Ocean colour remote sensing and *in situ* iceberg tracking. Deep-Sea Research I. 56, 1727-1741.

Smith Jr, W. O., Robison, B. H., Helly, J. J., Kaufman, R. S., Ruhl, H. A., Shaw, T. J., Twiming, B. S. & Vernet, M., 2007. Free-Drifting Icebergs: Hot Spots of Chemical and Biological Enrichment in the Weddell Sea. Science. 317, 478-482.

Wright, S. W. & van den Enden, R. L., 2000. Phytoplankton community structure and stocks in the East Antarctic marginal ice zone (BROKE survey, January-March 1996) determined by CHEMTAX analysis of HPLC pigment signatures. Deep-Sea Research II. 47, 2363-2400.

Zapata, M., Rodríguez, F. & Garrido, J. L., 2000. Separation of chlorophylls and carotenoids from marine phytoplankton: a new HPLC method using a reserved phase C_8 column and pyridine-containing mobile phases. Marine Ecology Progress Series. 195, 29-45.

Figure Captions

Figure 1. (A) Map of Antarctica showing the Antarctic Peninsula tip area. (B) Map of the Antarctic Peninsula showing the location of the study area. The marker represents the location of the tagged iceberg on 19 February 2009 (JRI, James Ross Island; AS, Antarctic Sound).

Figure 2. (A) 250 m resolution image derived from MODIS-Aqua on 20 February 2009; the icebergs and islands appear white and the water appears black. The red circle marks the iceberg position, which was tagged on 19 February (B) Radar image of the same day shows the tagged iceberg (Advanced Synthetic Aperture Radar [ASAR] from ENVISAT). The yellow points correspond to the hydrographic station positions in relation to the iceberg position.

Figure 3. (A) Surface chlorophyll-a concentration derived from MODIS-Aqua image for the study area on 20 February 2009. The red marker represents the initial location of the tagged iceberg. (B) Iceberg locations at the time we occupied the CTD stations. The numbers 1–6 denote the position of the iceberg when the corresponding CTD stations were occupied in the study area. Note that station #I201– #I203 (stations # I204–# I206) were located south (north) of the iceberg and it drifted northward.

Figure 4. Map of the study area with the track of the iceberg from the first day (19 February) to 1 June. The GPS positions of the tagged iceberg were acquired from ARGO satellite system.

Figure 5. Vertical profiles of temperature, salinity, and density. First column (left) shows stations south of the iceberg, and the second column (right) shows stations north of the iceberg.

Figure 6. (A) Diagram T/S for stations south of the iceberg and Station #I206, which was farther from the tagged iceberg and was not influence by freshwater of the melting iceberg. (B) Diagram T/S for stations located to the north of the iceberg (B). The T/S Diagram for the entire water column (~350 m).

Figure 7. Density profiles for the 2 stations were the furthest apart Station #I201 located south of the iceberg and Stations #I206 located north of the iceberg.

Figure 8. Vertical profiles of *in situ* stimulated fluorescence and beam attenuation coefficient (660nm). First column (left) shows stations south of the iceberg, and the second column (right) shows stations north of the iceberg.

Figure 9. Vertical profiles of nitrate, silicate and phosphate within the water column. First column (left) shows stations south of the iceberg, and the second column (right) shows stations north of the iceberg.

Figure 1

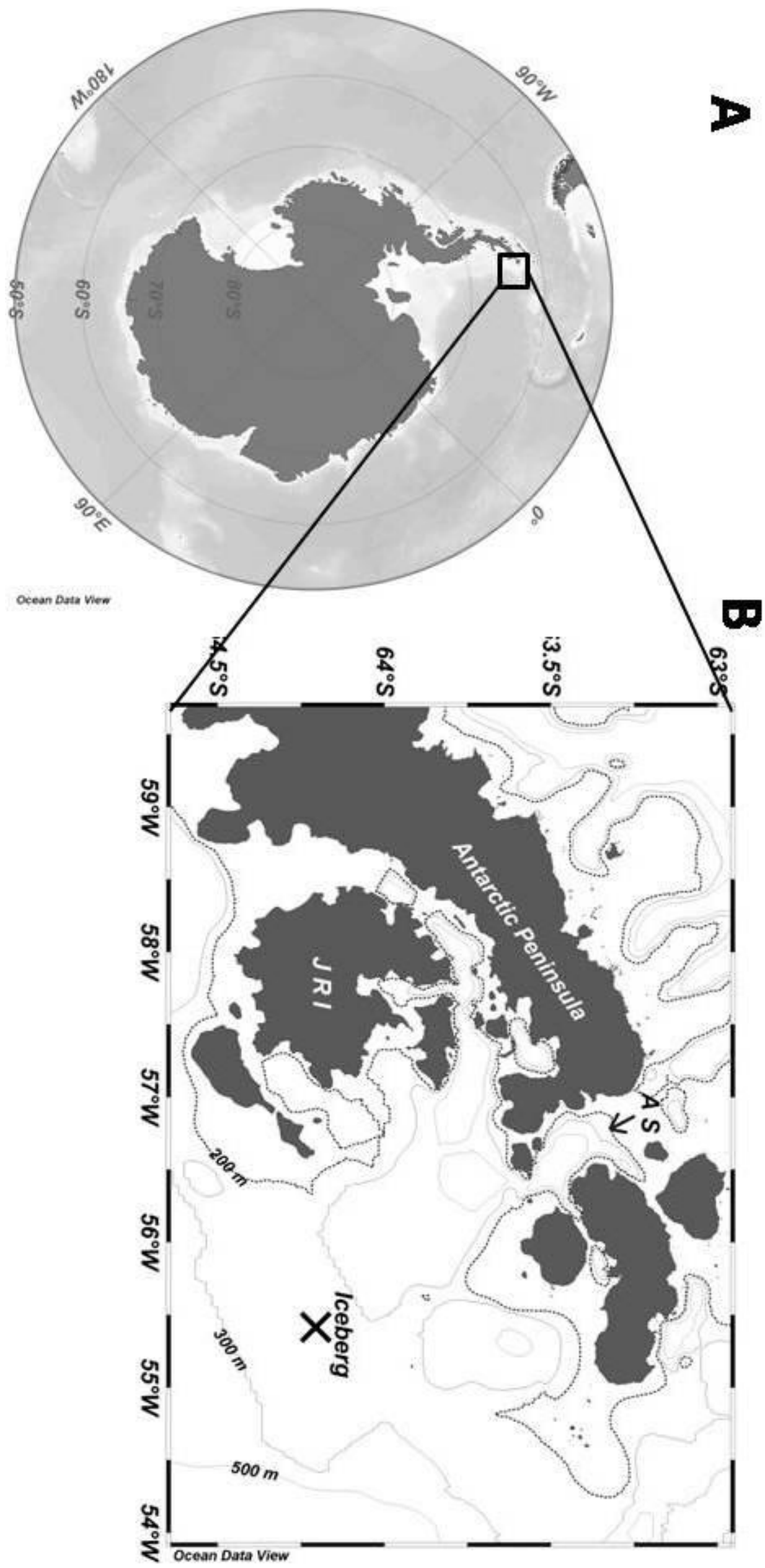
A
180°W
90°W
60°S
60°S
70°S
80°S
90°E
0
Ocean Data View
B
64°S
63°S
59°W
58°W
57°W
56°W
55°W
54°W
Antarctic Peninsula
J R I
A S
Iceberg
200 m
300 m
500 m
Ocean Data View

Figure 2

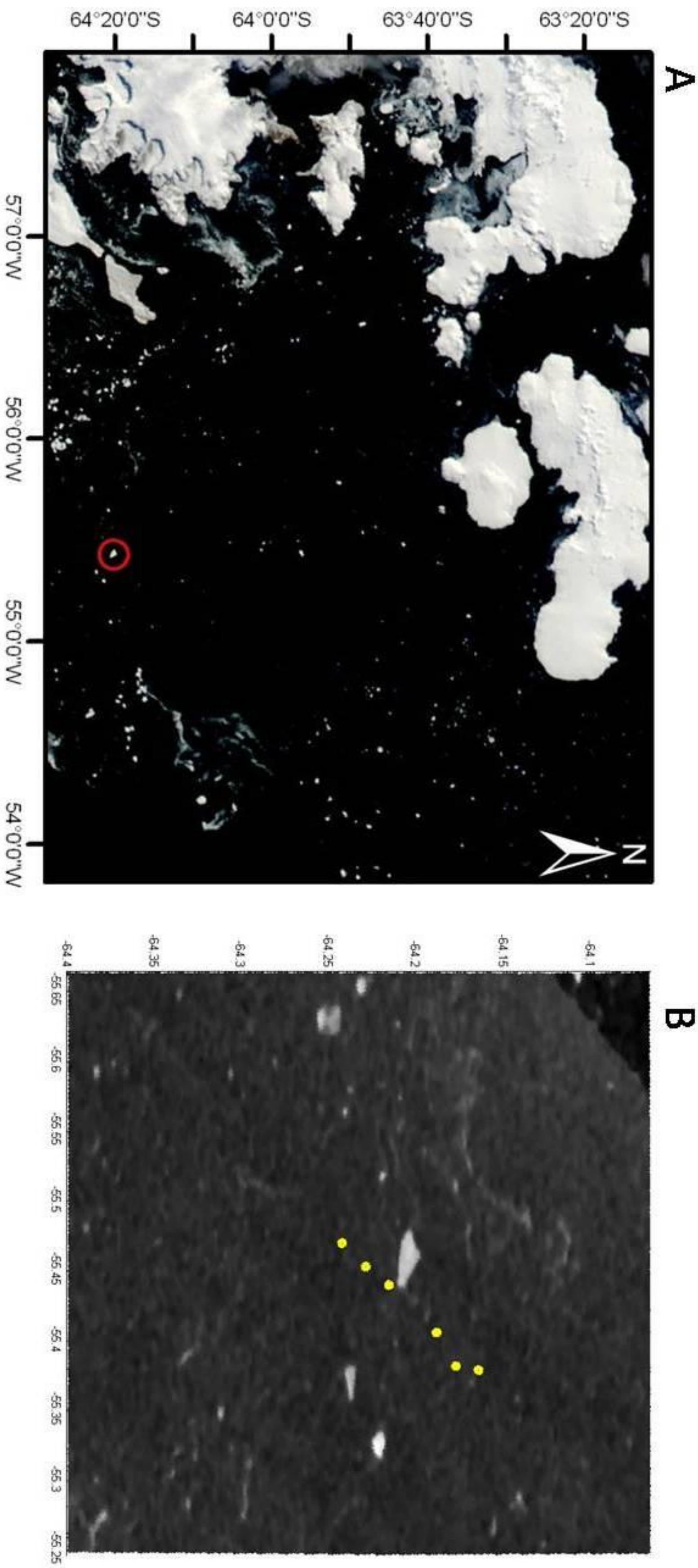

Figure 3

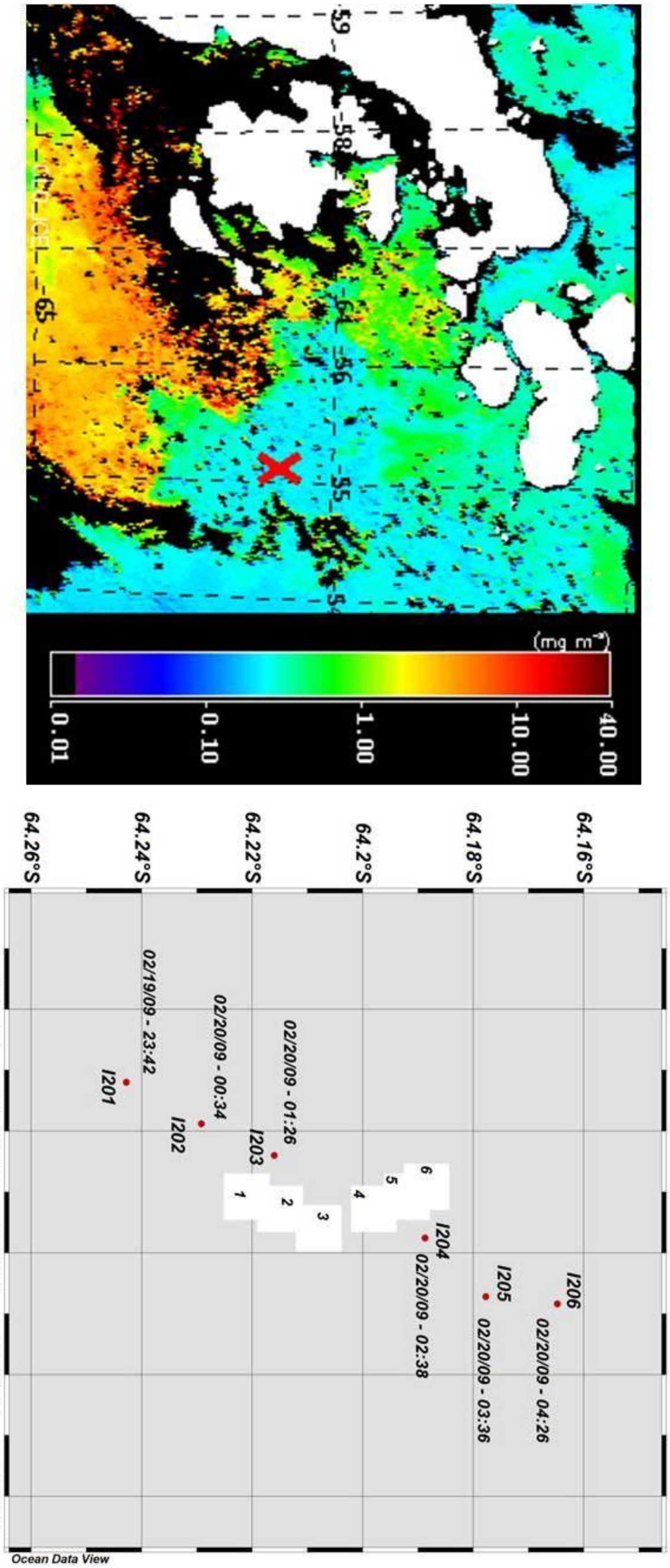

(mg m⁻³)
0.01
0.10
1.00
10.00
40.00
64.26°S
64.24°S
64.22°S
64.2°S
64.18°S
64.16°S
55.5°W
55.45°W
55.4°W
55.35°W
55.3°W
I201
02/19/09 - 23:42
I202
02/20/09 - 00:34
I203
02/20/09 - 01:26
I204
02/20/09 - 02:38
I205
02/20/09 - 03:36
I206
02/20/09 - 04:26
1
2
3
4
5
6
Ocean Data View

Figure 4

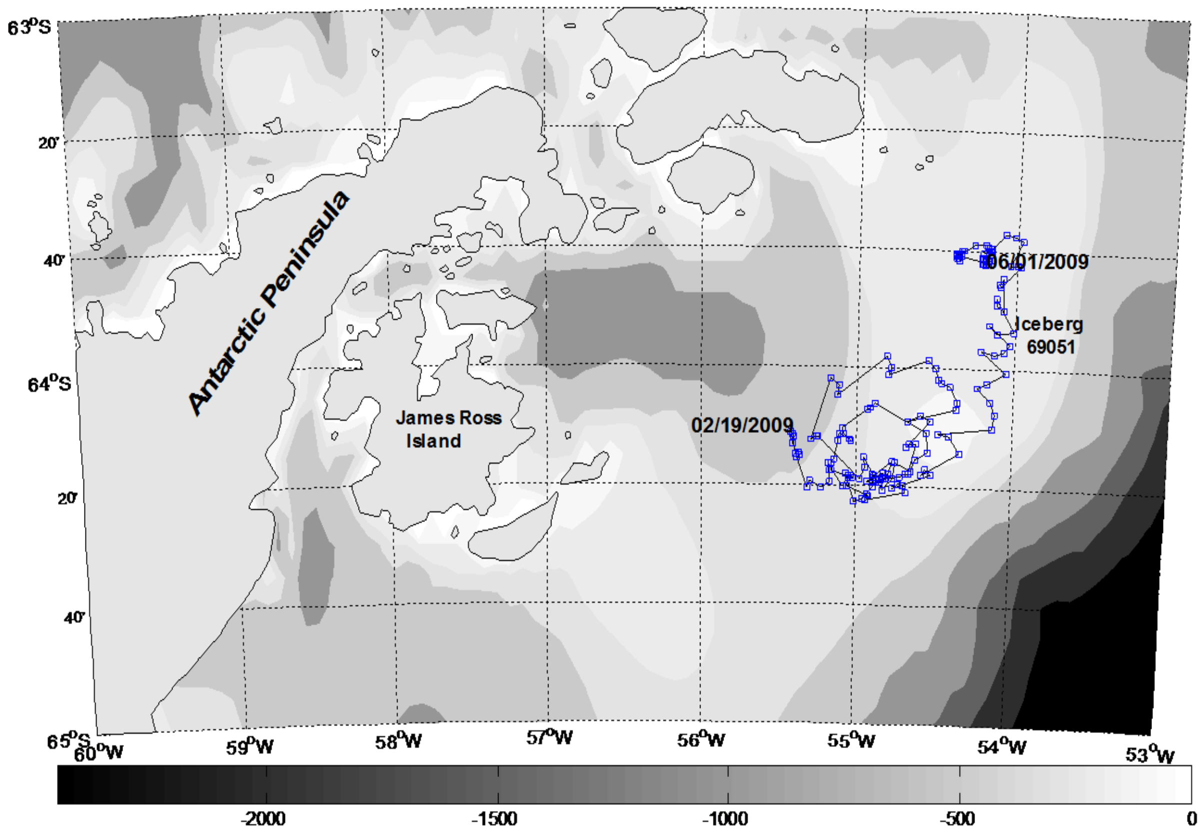

63°S
20'
40'
64°S
20'
40'
65°S
60°W
59°W
58°W
57°W
56°W
55°W
54°W
53°W
Antarctic Peninsula
James Ross
Island
02/19/2009
06/01/2009
Iceberg
69051
-2000
-1500
-1000
-500
0

Figure 5

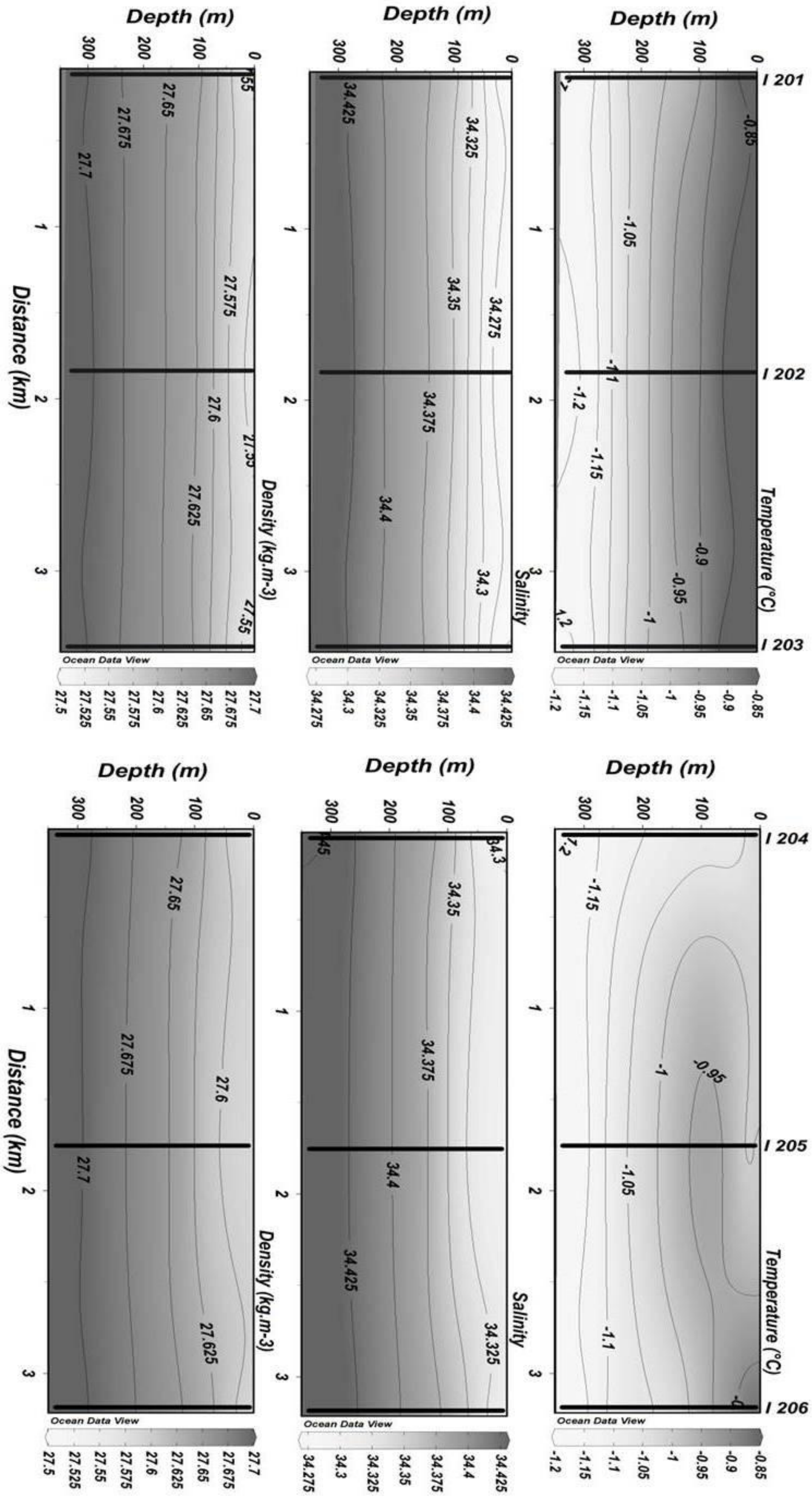
I 201
I 202
I 203
I 204
I 205
I 206
Depth (m)
Distance (km)
Temperature (°C)
Salinity
Density (kg.m-3)
Ocean Data View

Figure 6

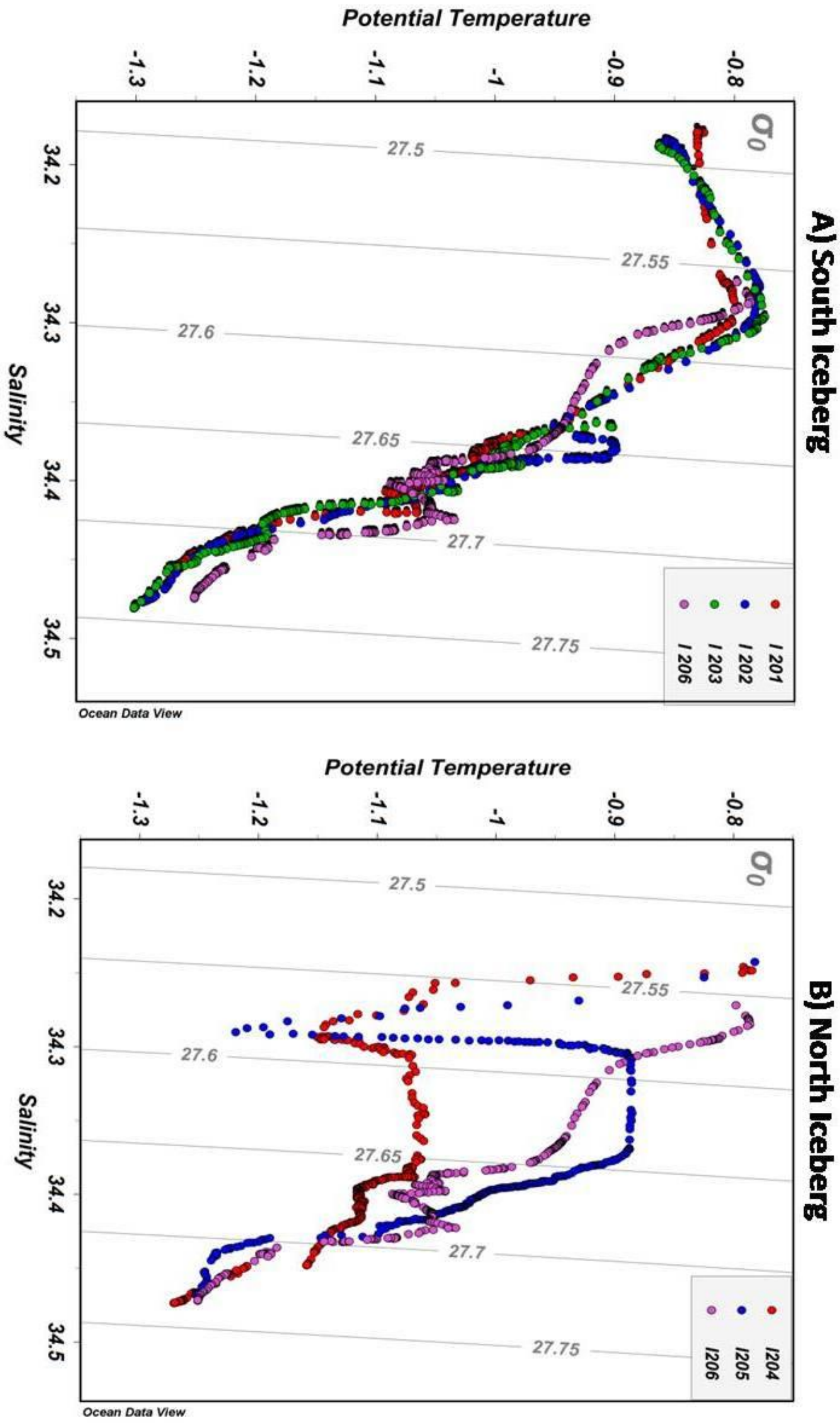
A) South Iceberg
Potential Temperature
Salinity
I 201
I 202
I 203
I 206
Ocean Data View
B) North Iceberg
Potential Temperature
Salinity
I204
I205
I206
Ocean Data View

Figure 7

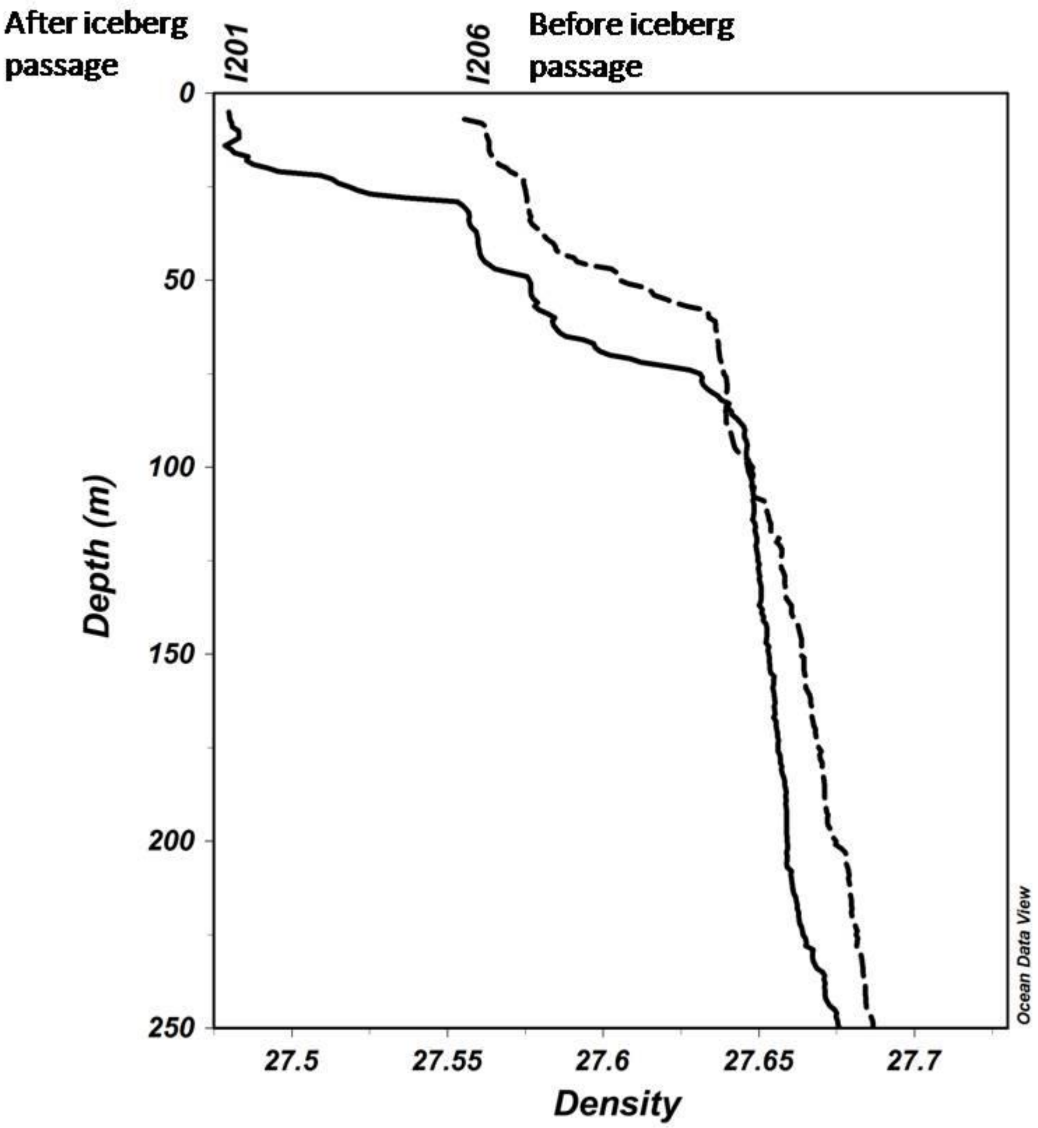
After iceberg passage
I201
I206
Before iceberg passage
0
50
100
150
200
250
Depth (m)
27.5
27.55
27.6
27.65
27.7
Density
Ocean Data View

Figure 8

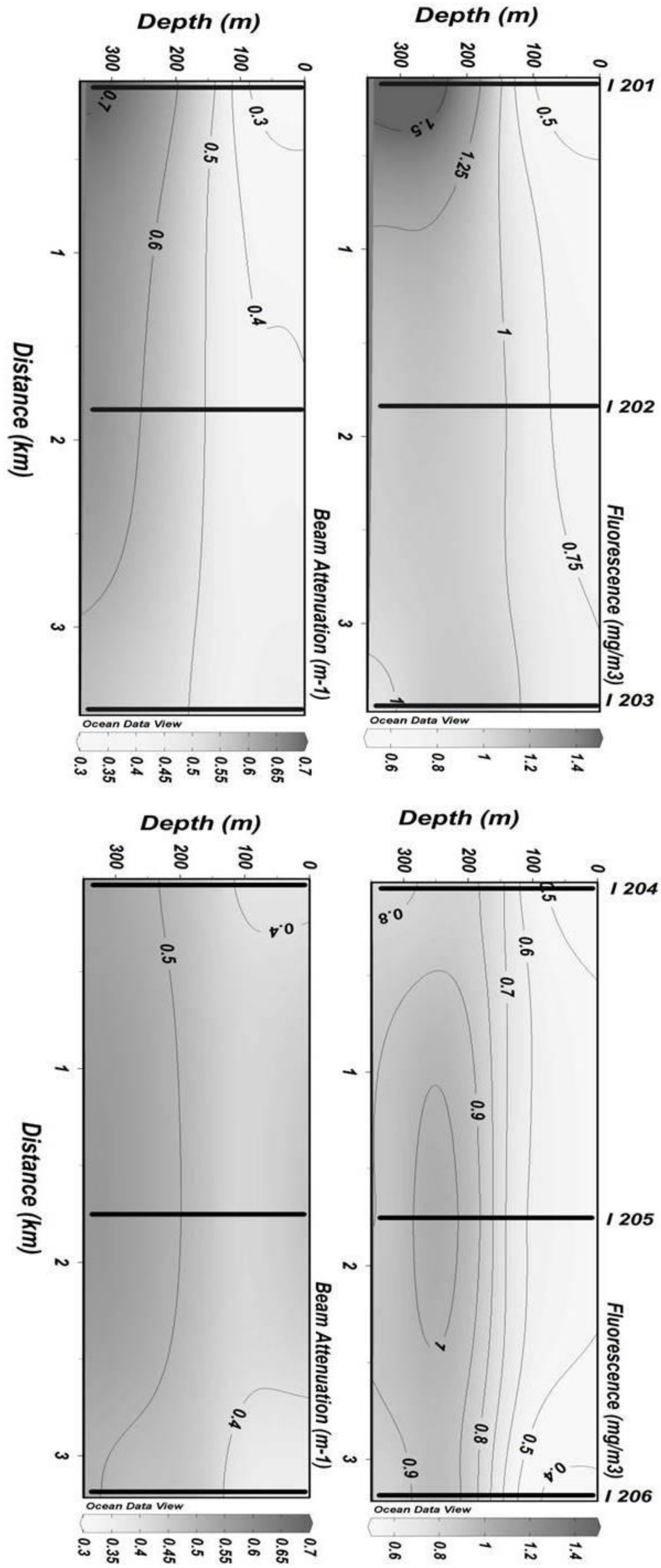
Depth (m)
Distance (km)
Fluorescence (mg/m3)
Beam Attenuation (m-1)
I 201
I 202
I 203
I 204
I 205
I 206
Ocean Data View

Figure 9

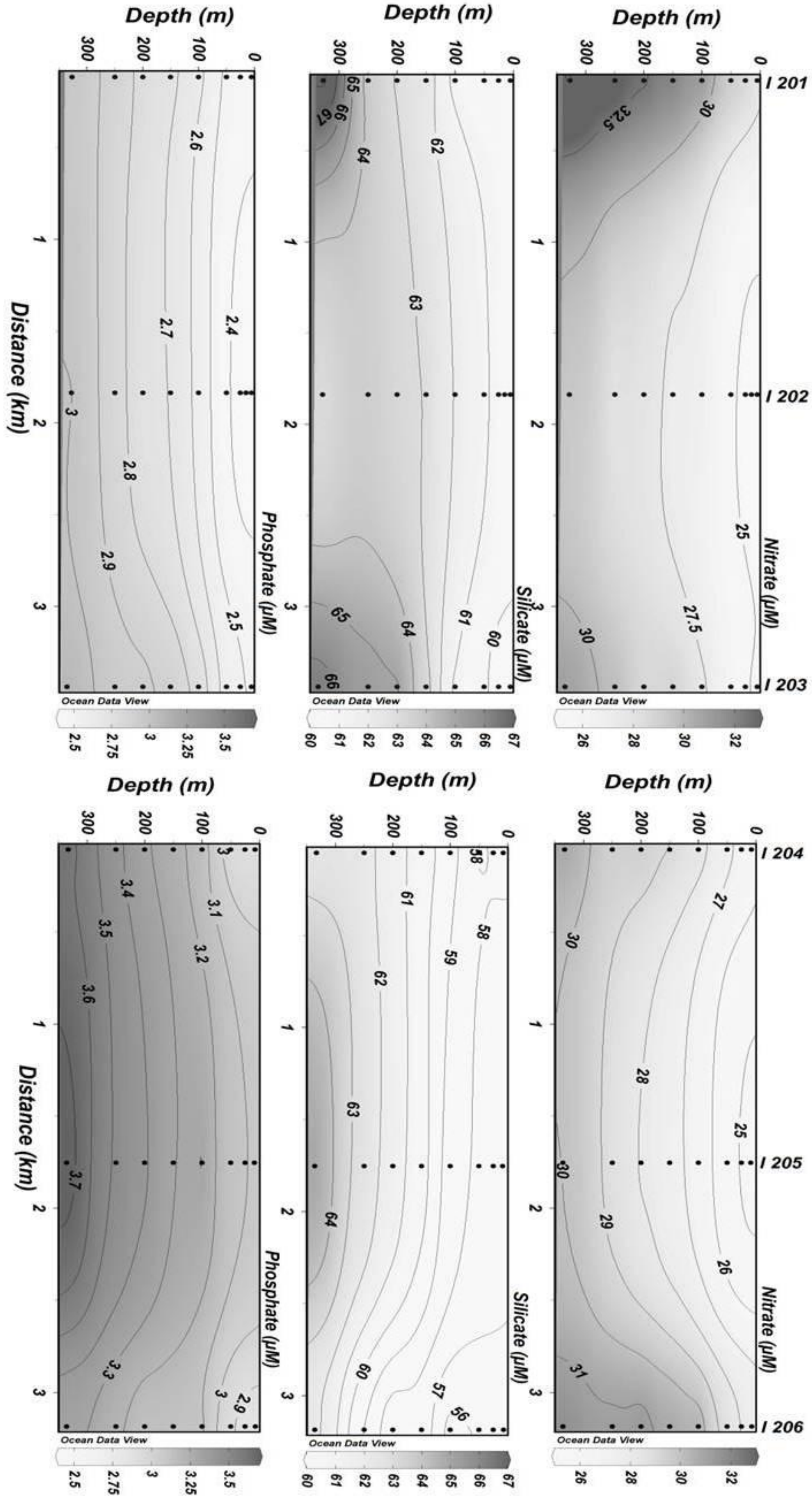
Depth (m)
Distance (km)
Nitrate (µM)
Silicate (µM)
Phosphate (µM)
I 201
I 202
I 203
I 204
I 205
I 206
Ocean Data View